

A theoretical investigation provides an integrated understanding of the complex regulatory network controlling *Arabidopsis* root hair patterning.

Author list

Hayley Mills¹, George Janes², Anthony Bishopp², Natasha Savage^{1*}

¹Institute of Systems, Molecular and Integrative Biology. University of Liverpool. UK.

²School of Biosciences. University of Nottingham. UK.

*nsavage@liverpool.ac.uk

Abstract

A complex regulatory network controlling *Arabidopsis* root hair patterning has been defined using data collected over decades by numerous labs. The network, embedded in the root epidermis contains a central regulation complex whose regulation is determined by positive and negative feedback loops, cell-cell signalling within the epidermal tissue, and positional signalling from underlying tissue. While there are extensive data regarding individual components and their interactions within the network, the complexity of the network has made it difficult to understand the sufficiency of the regulatory network to produce robust epidermal patterning, and how individual components and interactions contribute to correct epidermal patterning. To address these questions mathematical modelling was used to integrate the wealth of experimental data into one regulatory network model.

It was found that our current understanding of the epidermal patterning regulatory network was insufficient to reproduce experimental data. The model was used to hypothesise the existence of an additional negative feedback loop which, when added to the currently understood regulatory network, enabled the model to reproduce both wild type and mutant root hair patterning. Theoretical experiments on the modified regulatory network were used to; show that cooperativity or oligomerisation within the positive feedback loop is essential; define an essential relationship between the diffusive movement of two cell-cell signalling proteins; show that directed movement of another cell-cell signalling protein increased patterning robustness and that removal of directed that movement caused root hair patterning to appear as though it no longer receives positional cues. Theoretical results from the individual mechanistic experiments were analysed together to provide holistic understanding of the regulatory network.

This work presents an in-depth, integrated, exploration of the regulatory network controlling epidermal root hair patterning in *Arabidopsis*, and derives new insight into the roles of network components, and their combined mechanistic action.

1 Introduction.

Regulatory networks are used to illustrate and study the biological mechanisms responsible for controlling particular biological processes. Regulatory networks are often built to incorporate data accumulated by numerous groups. Practical constraints often lead to individual groups focussing on certain aspects of a regulatory network, resulting in subsets of network components and their interactions being studied in isolation from the rest of the network. Mathematical modelling is a tool with which one can integrate the distributed data generated by numerous groups, over many years. The resulting regulatory network model can be used to understand how network components work together to control the processes under scrutiny.

This study uses mathematical modelling to bring together the vast body of work which has uncovered components, and regulatory links, within the regulatory network responsible for *Arabidopsis* root epidermal patterning. While the components and interactions within the *Arabidopsis* root epidermal patterning network are well studied in isolation, their integrated ability to produce epidermal patterns is not clear. Here, published

data was used to build a mathematical model of the *Arabidopsis* regulatory network. The network model was then used to assess the sufficiency of our current knowledge to reproduce epidermal patterning. The model was also used to perform mechanistic investigations designed to examine the essential nature and functional limits of regulatory network interactions.

Arabidopsis root epidermal cells are arranged in longitudinal cell files. As *Arabidopsis* root epidermal cells immerse from the root apical meristem they differentiate into trichoblast (hair bearing) or atrichoblast (no hair) cell fates. Trichoblast, atrichoblast patterning is well described, with trichoblast cells forming in the epidermal cell files that touch an underlying cortical cleft, the cleft between two cortical cell files [1,2], Figure 1A. An epidermal cell overlying a cortical cleft is said to be in the H position. The arrangement of trichoblast cell files forming over cortical clefts has led to the hypothesis that a signal moves through the cortical cleft and is preferentially received by epidermal cells in the H position, biasing H position cell differentiation to promote trichoblast cell fate [3]. A cortical signal has yet to be identified.

Despite the simplicity of the trichoblast pattern, the regulatory network which controls epidermal cell fate specification in the *Arabidopsis* root does not take the form of a single pathway, where an upstream component, susceptible to cortical signalling, triggers a signalling cascade resulting in trichoblast cell fate. An abundance of data defining the *Arabidopsis* root epidermal regulatory network's architecture indicates that the network contains both positive and negative feedback loops as well as epidermal cell-cell signalling, Figure 1B.

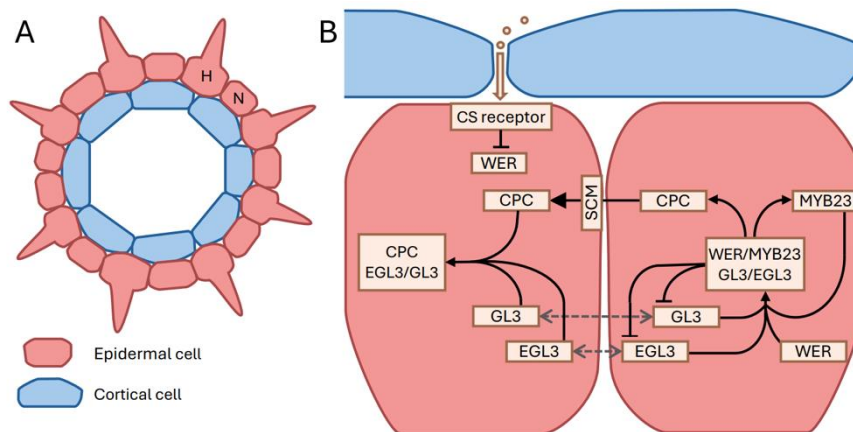


Figure 1: Epidermal and cortical layers in the *Arabidopsis* root. (A) Root cross section diagram. Epidermal cells touching two cortical cells are in the H position, other epidermal cells are in the N position. (B) The regulatory network in differentiated wild type epidermal cells. Black arrows represent promotion or complex formation, black barbed arrows represent repression. Diffusive movement between epidermal cells is shown as dashed, double headed, grey arrows. The cortical signal is represented as an arrow approaching the cortical signal (CS) receptor. Protein and mRNA are represented within one box.

At the centre of the regulatory network is a transcription factor complex which consists of, the MYB transcription factors WEREWOLF (WER) and MYB23, the basic helix-loop-helix transcription factors GLABRA3 (GL3) and ENHANCER OF GLABRA3 (EGL3), and a WD-repeat protein TRANSPARENT TESTA GLABRA1 (TTG1) [4–6,2]. The WER/MYB23 complex promotes the transcription of *GLABRA2* (*GL2*) [7–9]. *GL2* is a homeodomain-Zip transcription factor responsible for suppressing root hair growth and defining atrichoblast cell fate. Thus, the WER/MYB23 complex promotes atrichoblast cell fate and the WER, MYB23 proteins accumulate in epidermal cells which do not overlie a cortical cleft, referred to as N positions [4,5], Figure 1.

Data suggested that *WER* transcription was negatively regulated by a cortical signal via the leucine-rich repeat receptor-like kinase SCRAMBLED (SCM) [10]. It was proposed that the negative regulation of *WER* in H positions hindered the ability of the WER/MYB23 complex to form, promoting trichoblast cell fate. The role of SCM has since been revised, and SCM has been shown to have a role in epidermal cell-cell signalling [11]. Nonetheless, as trichoblast cells form in files over the cortical clefts, and the WER/MYB23 complex promotes atrichoblast cell fate, *WER* is still hypothesised to be negatively regulated by a cortical signal, although the signal and receptor for this signal are unknown.

In addition to promoting *GL2*, the WER/MYB23 complex regulates its own formation through positive and negative feedback loops. The WER/MYB23 complex promotes *MYB23* transcription [5]. The resulting MYB23

binds GL3, EGL3 and increases the concentration of WER/MYB23 complex, which goes on to promote MYB23 transcription, creating a MYB23 positive feedback loop. Despite the similarities between WER and MYB23, the WER/MYB23 complex does not regulate WER transcription [5,12]. The WER/MYB23 complex represses the transcription of GL3, EGL3 [13,5] to form one negative feedback loop. The WER/MYB23 complex also promotes the transcription of CAPRICE (CPC), which translates into a MYB-like protein, CPC [14,15]. CPC competes with WER/MYB23 to bind GL3, EGL3 and form the CPC complex, thus preventing WER/MYB23 complex formation [6,9], in another negative feedback loop.

There remains an open question regarding additional regulation on WER transcription. A modelling study showed that WER regulation, in addition to the cortical signal, was necessary for the modelled root epidermis to reproduce biological data, and suggested that WER transcription may be repressed by CPC [12]. However, the model in [12] was a probabilistic Boolean model which predated the discovery of MYB23 [5] and modelled SCM in its old role, as a cortical signal receptor [16]. An experimental study presented the hypothesis that there was no additional regulation on WER, that competitive binding of GL3/EGL3 by WER and CPC was sufficient to enable epidermal patterning [9]. The question of WER transcriptional regulation was addressed in this study. Here it was found that additional WER transcriptional regulation was necessary for correct epidermal patterning and a regulation mechanism was proposed.

CPC can move between epidermal cells and data suggests that this movement has a regulatory component [17]. Recently it has been shown that SCM facilitates the movement of CPC by importing CPC into the cell [11]. SCM has also been shown to be preferentially expressed in trichoblast cells, in the H position [18], and so SCM imports CPC into trichoblast cells from neighbouring atrichoblast cells. CPC translation is promoted in atrichoblast cells by the WER/MYB23 complex [14,15], wherein the resulting CPC protein competes with WER and MYB23 for GL3 and EGL3 binding. It seems likely then, that the directed removal of CPC, by SCM, from atrichoblast cells would promote correct epidermal patterning. In this study it is shown that SCM import of CPC decreases the differentiating epidermal cells' sensitivity to changes in reaction rates, making correct patterning more robust.

SCM was initially thought to be a cortical signal receptor because trichoblast cells became decoupled from the cortical cleft in *scm* mutants [16]. Now SCM's role has been redefined as a CPC importer [11], it is not clear that without any change to the epidermal cells' ability to perceive the cortical signal, removing CPC import would result in the *scm* mutant trichoblast, atrichoblast pattern. Within this study it is shown that the removal of CPC import alone is sufficient to account for the *scm* mutant pattern, the *scm* pattern can be reproduced without any change to the epidermal cells' ability to perceive the cortical signal.

GL3 can also move between epidermal cells [13] as can EGL3, although EGL3 movement has been reported to be restricted when compared to the movement of GL3 [19]. GL3, EGL3 movement between cells is hypothesised to be diffusive [12,20]. The WER/MYB23 complex represses GL3, EGL3 transcription enabling GL3, EGL3 concentration gradients which facilitate the diffusive movement of GL3, EGL3 from trichoblast cells to atrichoblast cells, wherein GL3, EGL3 become available to form the WER/MYB23 or CPC complex. It is not known what, if any, functional role the restriction of EGL3 movement has in epidermal patterning. In this study the necessity of EGL3 restricted movement is investigated and found to be essential for correct epidermal patterning. It is shown that EGL3 restricted movement, coupled with differential binding affinities during WER/MYB23 and CPC complex formation promote correct epidermal patterning.

Multiple binding sites have been reported on three reactions within the regulatory network, two of which appear within the MYB23 positive feedback loop. There are multiple binding for WER on the MYB23 promotor [5], WER on the CPC promotor [14,15], and multiple GL3, EGL3, WER, MYB23 proteins are reported to be involved in WER/MYB23 complex formation [9]. Cooperativity and oligomerisation impact reaction dynamics, producing reaction insensitivity at low reactant concentrations and nonlinear reaction rate increases with increasing reactant concentrations. This study shows that at least one multiple binding site reaction within the MYB23 positive feedback loop is essential for correct patterning, and suggests that the roles of multiple binding site reactions within the MYB23 positive feedback loop are to protect the regulatory network from noise driven patterning early in development, and to create switch like dynamics later in development as regulator concentrations increase.

These results presented here provide an in-depth, integrated, understanding of the regulatory network controlling *Arabidopsis* root hair patterning.

2 Methods.

2.1 Model Equations.

Terms within the differential equations were derived using either mass action kinetics or the Hill equation [21]. Models were solved numerically in MATLAB, using bespoke solvers. All code is available on GitHub [\[ref\]](#).

GL3, EGL3.

The dynamics of GL3, denoted g , and EGL3, denoted e , are governed by; basal transcription at rates b_g and b_e respectively, degradation at rates d_g and d_e , and repression of GL3, EGL3 transcription by the total concentration of WER/MYB23 complex [13,5], denoted A_T , Equation (18). The repression of GL3, EGL3 transcription by the total WER/MYB23 complex has been modelled as a GL3, EGL3 degradation term with degradation rates r_g , r_e , respectively.

$$\frac{d}{dt}g = b_g - r_g A_T g - d_g g \quad (1)$$

$$\frac{d}{dt}e = b_e - r_e A_T e - d_e e \quad (2)$$

GL3, EGL3.

GL3, denoted G , and EGL3, denoted E , diffuse between epidermal cells [13,19]. Diffusion is described using the standard Laplacian operator, Δ , with diffusion coefficients D_G for GL3 and D_E for EGL3. GL3, EGL3 translation takes place with rates q_G and q_E , respectively. GL3, EGL3 degradation takes place with rates d_G and d_E . Other reactions that affect the dynamics of GL3, EGL3 are those involved in WER/MYB23 complex and CPC complex formation and deformation [6,9]. It has been proposed that the WER/MYB23 complex contains at least two GL3/EGL3 and WER/MYB23 proteins [9]. To enable the effect of the number of GL3/EGL3 and WER/MYB23 proteins within the WER/MYB23 complex to be investigated, their number was chosen from a finite set of possibilities; $n_1 \in \{1,2,3,4\}$ for GL3, EGL3 and $n_2 \in \{1,2,3,4\}$ for WER, MYB23. Thus, $n_1 \in \{1,2,3,4\}$ GL3, EGL3 proteins are sequestered to WER/MYB23 complex formation and returned to the GL3, EGL3 pool on WER/MYB23 complex deformation. Because of lack of evidence to the contrary, one GL3, EGL3 protein is sequestered to CPC complex formation and returned on CPC complex deformation. W denotes WER, M denotes MYB23 and C denotes CPC. A_{GW} represents the WER complex containing GL3, A_{GM} represents the MYB23 complex containing GL3, A_{EW} represents the WER complex containing EGL3, and A_{EM} represents the MYB23 complex containing EGL3. I_{GC} and I_{EC} denote the CPC complexes containing GL3 and EGL3 respectively. k_{11} to k_{18} are reaction rates for WER/MYB23 complex formation and deformation, k_{21} to k_{24} are reaction rates for CPC complex formation and deformation.

$$\frac{\partial}{\partial t}G = q_G g - n_1 G^{n_1} (k_{11} W^{n_2} + k_{15} M^{n_2}) + n_1 (k_{12} A_{GW} + k_{16} A_{GM}) - k_{21} GC + k_{22} I_{GC} - d_G G + D_G \Delta G \quad (3)$$

$$\frac{\partial}{\partial t}E = q_E e - n_1 E^{n_1} (k_{13} W^{n_2} + k_{17} M^{n_2}) + n_1 (k_{14} A_{EW} + k_{18} A_{EM}) - k_{23} EC + k_{24} I_{EC} - d_E E + D_E \Delta E \quad (4)$$

WER.

WER concentration, denoted w , is increased by basal transcription, rate b_w . WER transcription is repressed by a cortical signal [3], denoted X , $X \in \{0,1\}$. $X = 1$ when the epidermal cell lies over a cortical cleft, $X = 0$ otherwise. It is hypothesised that the cortical signal is received by a receptor on the epidermal cell. Previous studies had proposed this receptor was SCM, as trichoblast cell fate was decoupled from the cortical cleft in roots without SCM [16]. Recently, the role of SCM in WER transcriptional regulation has been brought into question and data suggests that SCM functions to aid the movement of CPC between epidermal cells [11]. Nonetheless, positional signalling is still thought to be received by the epidermal cells. Thus, the model contains an unidentified cortical signal receptor, R_X . A previous modelling study suggested that WER transcription may be also be repressed by CPC [12]. Also investigated in this study is the repression of WER transcription by the total concentration of CPC complex, denoted I_T , Equation (19). Repression of WER transcription is modelled as WER degradation, r_{w21} is the rate at which the cortical signal represses WER

via R_X , and rates r_{w11} , r_{w12} are for the repression of WER by CPC and total CPC complex. WER has basal degradation rate d_w .

$$\frac{d}{dt}w = b_w - X(r_{w21}R_X)w - (r_{w11}C + r_{w12}I_T + d_w)w \quad (5)$$

MYB23.

$MYB23$, denoted m , transcription is promoted by total $WER/MYB23$ complex, A_T , Equation (18). There are four WER binding sites in the $MYB23$ promoter, one reported to have a more important role than the other three [5]. Thus, the number of $WER/MYB23$ complexes needed for $MYB23$ transcription was investigated, $n_3 \in \{1,2,3,4\}$. The mass action kinetics term to describe the total $WER/MYB23$ complex promotion of $MYB23$ transcription was, $p_m A_T^{n_3}$, where p_m is the transcription rate. It was found that using mass action kinetics for transcriptional promotion resulted in an unlikely $MYB23$ concentration amplification for $n_3 > 1$, data not shown. Thus, the Hill equation [21], rather than mass action kinetics, was used to describe total $WER/MYB23$ complex promotion of $MYB23$ transcription. The Hill coefficient is a measure of cooperativity between binding sites, with a maximum value equalling the number of available binding sites [22]. Thus, the Hill coefficient for $MYB23$ transcriptional was set to $n_3 \in \{1,2,3,4\}$. The maximum rate of $MYB23$ transcription was denoted p_m . K_m represents dissociation constant, as derived by mass action kinetics.

$$\frac{d}{dt}m = p_m \frac{A_T^{n_3}}{K_m + A_T^{n_3}} - d_m m \quad (6)$$

WER, MYB23.

WER , $MYB23$ translation takes place with rates q_W and q_M , and degradation with rates d_W and d_M , respectively. $n_2 \in \{1,2,3,4\}$ WER and $MYB23$ proteins are sequestered during the formation of the $WER/MYB23$ complex and gained when the $WER/MYB23$ complex disassociates [9].

$$\frac{d}{dt}W = q_W W - n_2 W^{n_2} (k_{11}G^{n_1} + k_{13}E^{n_1}) + n_2 (k_{12}A_{GW} + k_{14}A_{EW}) - d_W W \quad (7)$$

$$\frac{d}{dt}M = q_M M - n_2 M^{n_2} (k_{15}G^{n_1} + k_{17}E^{n_1}) + n_2 (k_{18}A_{EM} + k_{16}A_{GM}) - d_M M \quad (8)$$

CPC.

CPC , denoted c , transcription is promoted by total $WER/MYB23$ complex [14,15]. Three distinct WER binding sites have been found on the CPC promotor, each with different affinities to WER but all were required for proper gene expression [14,15]. Thus, the number of $WER/MYB23$ complex needed to promote CPC transcription was chosen from the set $n_4 \in \{1,2,3\}$. To prevent a biologically unlikely CPC concentration amplification caused by using mass action kinetics to describe total $WER/MYB23$ complex promotion of CPC transcription (data not shown), the Hill equation [21] was used, with Hill coefficient $n_4 \in \{1,2,3\}$. The maximum rate of CPC transcription was denoted p_c and K_c represents the dissociation constant.

$$\frac{d}{dt}c = p_c \frac{A_T^{n_4}}{K_c + A_T^{n_4}} - d_c c \quad (9)$$

CPC.

CPC translation rate was denoted q_C , and degradation rate denoted d_C . CPC concentration is increased when the CPC complex disassociates and decreased when it is formed [6,9]. CPC can move between epidermal cells [17]. Data suggests that SCM , denoted S , acts to facilitate the import of CPC [11]. The movement of CPC was described by two terms, diffusion with diffusion coefficient D_C , and SCM import with proportionality constant \tilde{D}_C . CPC diffusion was calculated using the Laplacian operator and SCM import was calculated using a finite difference scheme, Equation (11), i is the epidermal cell index, C_i is the concentration of CPC in cell i , S_i the concentration of SCM in cell i . As SCM has been shown to localise in cells in the H position [18], SCM $S_i = 1$ when the epidermal cell lies over a cortical cleft, 0 otherwise.

$$\frac{\partial}{\partial t}C = q_C C + k_{22}I_{GC} + k_{24}I_{EC} - (k_{21}GC + k_{23}EC) - d_C C + \tilde{D}_C f(C, S) + D_C \Delta C \quad (10)$$

$$f(C, S) = (S_i(C_{i+1} + C_{i-1}) - C_i(S_{i+1} + S_{i-1})) \quad (11)$$

WER/MYB23 complex.

$$\frac{d}{dt}A_{GW} = k_{11}G^{n_1}W^{n_2} - k_{12}A_{GW} \quad (12)$$

$$\frac{d}{dt}A_{EW} = k_{13}E^{n_1}W^{n_2} - k_{14}A_{EW} \quad (13)$$

$$\frac{d}{dt}A_{GM} = k_{15}G^{n_1}M^{n_2} - k_{16}A_{GM} \quad (14)$$

$$\frac{d}{dt}A_{EM} = k_{17}E^{n_1}M^{n_2} - k_{18}A_{EM} \quad (15)$$

CPC complex.

$$\frac{d}{dt}I_{GC} = k_{21}GC - k_{22}I_{GC} \quad (16)$$

$$\frac{d}{dt}I_{EC} = k_{23}EC - k_{24}I_{EC} \quad (17)$$

Total WER/MYB23 and CPC complexes.

As MYB23 can functionally replace WER [5] and GL3, EGL3 are functionally similar [6,13,23] total WER/MYB23 complex, Equation (18), was used within the relevant differential equations. Similarly, for the CPC complexes and total CPC complex was used, Equation (19).

$$A_T = A_{GW} + A_{EW} + A_{GM} + A_{EM} \quad (18)$$

$$I_T = I_{GC} + I_{EC} \quad (19)$$

2.2 Parameter Search.

There are a lack of data measuring the rates of reactions within the regulatory network controlling *Arabidopsis* root epidermal patterning. A random search approach was chosen to explore the ability of the model to reproduce biological data.

Thirty-eight core parameters were defined, Table 1. A core parameter set was defined as thirty-eight parameter values, one for each core parameter. 20,000 core parameter sets were chosen uniformly at random from the arbitrary interval (0,10]. Core parameter sets were indexed 1 to 20,000 and fixed. i.e core parameters define rates for reactions which remained unchanged for all modelling investigations. The values of thirteen additional parameters were set depending on the mechanistic investigation being undertaken, Table 2.

Table 1. Core parameters. Core parameter names and descriptions. 20,000 core parameter sets were chosen uniformly at random from the interval (0,10]. j is the index used to identify each core parameter during univariate sensitivity analysis (Section 2.3).

j		WER/MYB23 complex formation and deformation
1	k_{11}	A_{GW} association
2	k_{12}	A_{GW} disassociation
3	k_{13}	A_{EW} association
4	k_{14}	A_{EW} disassociation
5	k_{15}	A_{GM} association
6	k_{16}	A_{GM} disassociation
7	k_{17}	A_{EM} association
8	k_{18}	A_{EM} disassociation
		CPC complex formation and deformation
9	k_{21}	I_{GC} association
10	k_{22}	I_{GC} disassociation
11	k_{23}	I_{EC} association
12	k_{24}	I_{EC} disassociation
		basal degradation
18	d_G	GL3 protein
19	d_E	EGL3 protein
20	d_C	CPC protein
21	d_W	WER protein
22	d_M	MYB23 protein
23	d_g	GL3 mRNA
24	d_e	EGL3 mRNA
25	d_c	CPC mRNA
26	d_w	WER mRNA
27	d_m	MYB23 mRNA

j		basal transcription
15	b_g	GL3 mRNA
16	b_e	EGL3 mRNA
17	b_w	WER mRNA
		maximum transcription rate
33	p_c	CPC mRNA
34	p_m	MYB23 mRNA
		disassociation constant
38	K_c	WER on CPC transcript
37	K_m	WER on MYB23 transcript
		transcriptional repression
35	r_g	GL3 by WER/MYB23 complex
36	r_e	EGL3 by WER/MYB23 complex
		translation
28	q_G	GL3 protein
29	q_E	EGL3 protein
30	q_C	CPC protein
31	q_W	WER protein
32	q_M	MYB23 protein
		protein movement
13	D_G	GL3 diffusion
14	D_C	CPC diffusion

Table 2. Parameters changed during mechanistic investigations. Parameter names, descriptions and intervals from which parameter values were chosen. Parameters were set depending on the mechanistic investigation being undertaken. Descriptions of mechanistic investigations are given in the sections indicated at the top of each parameter column. For each of the 20,000 core parameter sets, the parameters n_1 , n_2 , n_3 and n_4 were either chosen uniformly at random from the set shown. When parameter intervals are given the parameter was chosen uniformly at random from the interval, for each of the 20,000 core parameter sets.

		§ 3.1	§ 3.4	§ 3.5
	number of proteins in WER/MYB23 complex			
n_1	GL3, EGL3	{2,3,4}	Table 7.	{2,3,4}
n_2	WER, MYB23	{2,3,4}	Table 7.	{2,3,4}
	number of binding sites on transcript			
n_3	WER on MYB23	{2,3,4}	Table 7.	{2,3,4}
n_4	WER on CPC	{2,3}	Table 7.	{2,3}
	WER transcriptional repression			
r_{w11}	by CPC	Table 5.	Table 5.	Table 5.
r_{w12}	by CPC complex	Table 5.	Table 5.	Table 5.
	EGL3 movement			
D_E	diffusion	0	0	(0,10]
	SCM function			
S	SCM	1, SCM+ 0, SCM-		
\tilde{D}_C	CPC import via SCM	(0,10]		
	Cortical signal input			
R_X	unknown receptor	(0,0.25]		
r_{w21}	WER repression via R_X	(0,10]		

Steady state solutions of models which included SCM, referred to as SCM+ models, were compared to wild type (WT) data. Steady state solutions of models which did not include SCM, referred to as SCM- models, were compared to *scm* mutant data. Biological data regarding the location of transcript and proteins were imaging data. Thus, the data indicates the total proteins in a cell, not whether those proteins are in a complex or not. For SCM+ model solutions, *in-silico* trichoblast cells were defined as having a steady state solution with high concentrations of total CPC [17], GL3, EGL3, total EGL3 [6,19] and low concentrations of total GL3 [13], WER, total WER [4], MYB and total MYB [5], when compared to atrichoblast cells. *In-silico* atrichoblast cells were defined as having a steady state solution with high concentrations of total GL3, WER, total WER, MYB and total MYB, and low concentrations of, total CPC, GL3, EGL3, total EGL3 when compared to trichoblast cells, Figure 1B. A threshold was applied such that, for a concentration difference between two cells to be considered significant the difference had to be over 10%.

For WT data trichoblast cells generally form in single files over the cortical cleft, thus it can be assumed that regulatory network components which have this pattern are co-localised in the trichoblast cell. A similar argument can be made for atrichoblast regulatory network components. As cell fate is decoupled from the cortical cleft in *scm* mutant roots, regulatory network component co-localisation cannot be assumed. For SCM- model solutions the *in-silico* WER/MYB complex (used as a GL2 proxy), total WER and CPC were compared to positional data for various trichoblast, atrichoblast markers [16,10,9,24,11,25].

A parameter set was labelled successful if both, the steady state solutions of the SCM+ model could reproduce WT data, and steady state solutions of the SCM- model could reproduce *scm* mutant data, Table 3. The WT data in Table 3 was generated by analysing twenty-three images of root cross-sections containing a GL2 reporter, Figure 2A. *scm* mutant data was taken from publications. *scm* mutant trichoblast, atrichoblast, positional data was available in table form [10,9,24,11,25], however the standard deviations in the published tables were much smaller than those calculated using model solutions and analysing published images. Thus, *scm* mutant data was calculated from eleven figures within six publications [16,10,9,24,11,25], Table 3 (S1

File). The means calculated using the published imaging data were comparable to the published tabulated means.

Table 3. WT and *scm* mutant cell type and position data. Percentage of each epidermal cell type in the H and N positions. Full data set in S1 File.

	H position		N position	
	trichoblast	atrachoblast	trichoblast	atrachoblast
WT	93.7 ± 8.4	6.3 ± 8.4	1.2 ± 3.0	98.8 ± 3.0
<i>scm</i>	61.8 ± 12.9	38.2 ± 12.9	22.4 ± 15.2	77.6 ± 15.2

The parameter test protocol for each of the 20,000 core parameter sets, for each mechanistic combination under investigation, had three steps. Consider an arbitrary parameter set, P_i , where P_i is a list of parameter values for each of the parameters shown in Tables 1 and 2. Recall, a parameter set was labelled successful if both the steady state solutions of the SCM+ model could reproduce WT data and steady state solutions of the SCM- model could reproduce *scm* mutant data, Table 3. The SCM and cortical signal receptor parameter values for the three parameter test steps are shown in Table 4.

Step 1: Solve the SCM+ model with zero initial conditions, using parameter set P_i . If the solution of the SCM+ model, with zero initial conditions and P_i , was such that all *in-silico* trichoblast cells were in the H position and all *in-silico* atrichoblast cells were in the N position then parameter set P_i was used in step 2. Otherwise, P_i was considered unsuccessful and discarded.

Step 2: Create the SCM- model and attempt to fit model solutions to *scm* mutant data, Table 3. Data shows that trichoblast cells are decoupled from the cortical cleft in *scm* mutant roots. Nonetheless trichoblast cells remain more likely to occupy the H position than atrichoblast cells, Table 3. To fit SCM- model solutions to *scm* mutant data the cortical signal receptor strength, R_X , and magnitude of the random initial conditions was incrementally changed. The *in-silico* cortical signal receptor strength was set within the interval $R_X \in (0, 0.25]$. The random initial conditions were such that, every component of the model, whose dynamics were described by a differential equation, was assigned an initial concentration, C_0 , chosen uniformly at random from a given interval, $C_0 = (0, C_{0_{max}}]$, $C_{0_{max}} \leq 1$. For each attempted fit, twenty SCM- solutions were generated and compared to *scm* mutant data, Table 3, using Welch's t-test. If the comparison resulted in a p-value greater than 0.05 then *in-silico* and *in-planta* data were not significantly different and parameter set P_i was labelled as a successful parameter set. If no successful fit could be found, parameter set P_i was considered unsuccessful and discarded. If a successful fit was found, parameter set P_i was used in step 3.

Step 3: Solve the SCM+ model with random initial conditions and receptor strength fitted using the SCM- model and compare solutions to data. The SCM+ model was solved twenty times and compared to WT data, Table 3, using Welch's t-test. If the comparison resulted in a p-value greater than 0.05 then *in-silico* and *in-planta* data were not significantly different and parameter set P_i was labelled as a successful parameter set.

Table 4. SCM and cortical signal receptor parameter values for the three parameter test steps.

	initial conditions	SCM, S	receptor, R_X
Step 1: SCM+	zero	1	1
Step 2: fit SCM-	random = (0,1]	0	(0,0.25]
Step 3: SCM+	random = (0,1]	1	(0,0.25]

All parameter sets can be found on GitHub [\[ref\]](#).

2.3 Univariate Sensitivity Analysis.

Univariate sensitivity analysis protocol. Univariate sensitivity analysis was performed on successful parameter set P_i . The values of each of the core parameters within P_i , labelled $j = \{1, 2, \dots, 38\}$, Table 1, were changed one by one. The mechanistic parameters within P_i , Table 2, were not changed during sensitivity analysis, as those parameters define specific mechanisms under scrutiny and to change them would be to change the mechanism. Consider core parameter $p_{i,j}$. During univariate sensitivity analysis the value of $p_{i,j}$ was multiplied by 10^x , for $x = \{-2, -1.75, -1.5, \dots, 2\}$ to give the perturbed parameter $p'_{i,j}$. For each perturbed parameter, $p'_{i,j}$, the SCM+ and SCM- models were solved twenty times, each with different noisy initial

conditions. The model solutions were then compared with experimental data, Table 3. The success or failure of the model solution, solved with parameter set P_i , containing the perturbed parameter $p'_{i,j}$, was recorded. An insensitive region for core parameter $p_{i,j}$ was defined as $r_{i,j} = x_{max} - x_{min}$, where x_{min} was the minimum value of x for which the model solved with parameter set P_i , containing the perturbed parameter $p'_{i,j}$ was a success, and x_{max} was the maximum value of x for which the model solved with parameter set P_i , containing the perturbed parameter $p'_{i,j}$, was a success. Sensitivity analysis code can be found on GitHub [\[ref\]](#).

2.4 Experimental Methods.

Plant Materials.

Wildtype *Arabidopsis* (Col-0) and *scm-2* mutants (SALK 086357) were obtained from the Nottingham *Arabidopsis* stock centre (NASC). Sterile seeds were sown onto 1% agar plates containing 0.5x Murashige and Skoog salts at pH 5.7. Plates were then stratified at 4°C for 48h before being moved to growth rooms set at 21°C and a 16 hour day length.

Molecular cloning and plant transformation.

Arabidopsis thaliana GLABRA2 (AT1G79840) genomic coding sequence was cloned from genomic DNA using primers designed according to the Greengate cloning system protocol [26]. The GLABRA2 coding sequence was cloned with a silent site-directed mutagenesis (V438V) to remove an internal BsaI site. mTurquoise was cloned from an existing plasmid with primers which include a glycine-serine (Gly-Ser) linker (GSSGGGSGGGGS) at the N-terminal end. The GL2 promoter was cloned and described previously [27]. Restriction and ligation reactions were performed using BsaI and T4 DNA ligase (New England Biolabs, MA, USA). All entry plasmids were confirmed for presence of an insert by colony PCR and Sanger or Oxford Nanopore sequencing (Source Bioscience, Cambridge, UK). The entry vectors were used to generate an expression vector with GL2 fused with mTurquoise at the C-terminus under the control of GL2 promoter (S2 File). Other components of the construct were derived from the Greengate kit described by Lampropoulos *et al.* (2013). This kit is available from Addgene (Kit #1000000036). The construct was assembled in the pGGZ001 Greengate destination vector (S2 File). Greengate assembly reactions were performed using NEB Golden Gate Cloning Kit (New England Biolabs, MA, USA). Final expression constructs were confirmed by colony PCR, restriction digest and Oxford Nanopore sequencing.

The expression vector was transformed into *Agrobacterium tumefaciens* by electroporation transformation in combination with pSOUP, which is necessary for proper replication of the pGREEN-based plasmid. *A. tumefaciens* colonies were selected using colony PCR for presence of the expression vector. These were cultured and then used to transform *Arabidopsis thaliana* plants via the floral dip method [28]. The construct was transformed into Columbia 0 background and *scm-2* (SALK_086357; insertion at *SCRAMBLED/STRUBBELLIG* AT1G11130; [16]). Transformant plants were selected for using hygromycin resistance.

Imaging and image processing.

5-day old seedlings were fixed with 4% paraformaldehyde in phosphate-buffered saline pH7.4 and cleared according to the Clearsee method [29], staining for 1h with Direct Red 23 (Sigma Aldrich) during clearing as described by Ursache *et al.* (2018) [30]. After clearing the root tips were mounted on slides and imaged on a Leica SP8 confocal microscope. Direct red 23 was excited using a 561nm laser line and detected at 580-615nm. mTurquoise was excited using a 442nm laser line and detected at 450-518nm. Data was processed using FIJI (ImageJ) and cell identity counts based on presence or absence of GLABRA2 protein estimated by mTurquoise signal.

3 Results.

3.1 The regulatory network model can reproduce WT and scm epidermal patterning if repression of WER is colocalised with the CPC complex.

To understand if the most up to date published reactions were sufficient to enable *in-silico* trichoblast patterning that matched biological data, the mechanistic parameters shown in Table 2 were set such that the equations modelled; SCM as a CPC importer, EGL3 restricted movement, cooperativity on MYB23 and CPC transcription and oligomerisation within the WER/MYB23 complex. WER transcription is directly repressed by the cortical signal. Whether or not WER transcription is also directly repressed by components within the regulatory network is not clear. A previous modelling study suggested that WER transcription may be also be repressed by CPC [12]. The model in [12] was a probabilistic Boolean model which predated the discovery of MYB23 and modelled SCM as a cortical signal receptor, as was the theory at the time. An experimental study presented the hypothesis that there was not additional regulation on WER, that competitive binding of GL3/EGL3 by WER and CPC was sufficient to enable epidermal patterning [9]. Both published mechanisms were investigated using the model, Table 2, column §3.1, Table 5. The different forms of Equation (5), the equation describing WER concentration dynamics, are shown in Table 6. None of the 20,000 core parameter sets could reproduce the biological data, for either of the mechanisms. Thus, competitive binding alone is insufficient to enable *Arabidopsis* root epidermal patterning. WER transcriptional repression by CPC was also inadequate to enforce the correct patterning *in-silico*. This is perhaps unsurprising as CPC translation is promoted by the WER/MYB23 complex and CPC translation is colocalised with the WER/MYB23 complex. Thus, when unbound CPC repressed WER translation in the model it hindered the ability of the WER/MYB23 complex to become dominant.

Table 5. Mechanistic parameter intervals for WER transcriptional repression investigation. CS stands for cortical signal. Other parameter intervals are shown in Tables 1 and 2.

parameter descriptions		parameter values for each mechanism		
	WER transcriptional repression	CS only	CS & CPC	CS & CPC complex
r_{w11}	by CPC	0	(0,10]	0
r_{w12}	by CPC complex	0	0	(0,10]

Table 6. Forms of Equation (5) in the WER transcriptional repression investigation.

Equation (5)	
General form	$\frac{d}{dt}w = b_w - X(r_{w21}R_X)w - (r_{w11}C + r_{w12}I_T + d_w)w$
CS only	$\frac{d}{dt}w = b_w - X(r_{w21}R_X)w - d_w w$
CS & CPC	$\frac{d}{dt}w = b_w - X(r_{w21}R_X)w - (r_{w11}C + d_w)w$
CS & CPC complex	$\frac{d}{dt}w = b_w - X(r_{w21}R_X)w - (r_{w12}I_T + d_w)w$

It was hypothesised that successful patterning may be achieved if WER transcription was repressed by a regulatory network component which dominated in trichoblast cells. WER had been shown not to positively regulate its own transcription [5,12], thus, the CPC complex was chosen and the repression of WER transcription by the CPC complex was tested.

For the model with WER translational repression by the cortical signal and CPC complex ten successful parameter sets were found out of the 20,000 tested, Figure 2B, S3 File. The WER repression by CPC complex model could reproduce the nonuniform trichoblast spacing seen in WT and scm mutant root cross-sections.

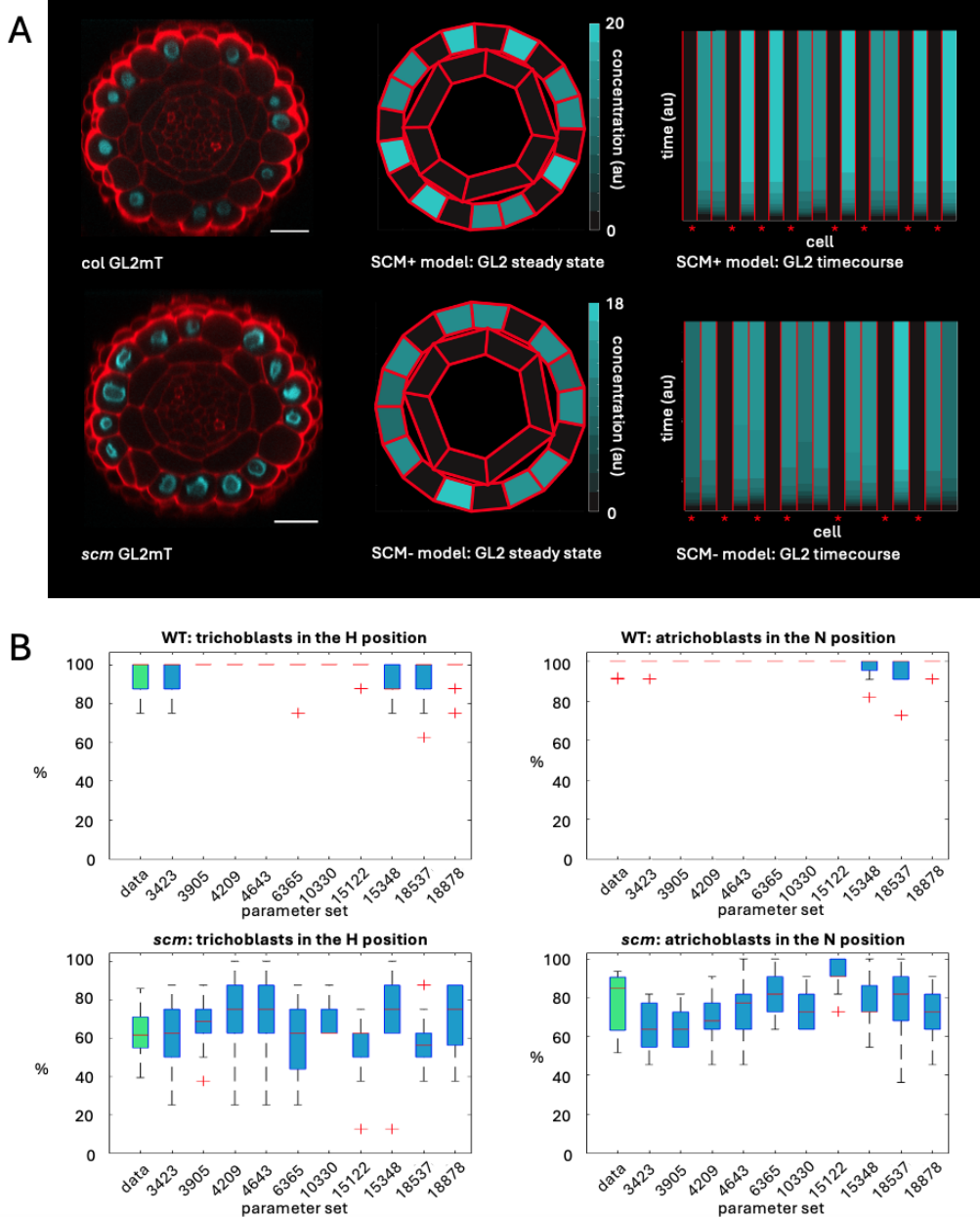


Figure 2: Comparing results of the SCM+ and SCM- models, with *WER* transcriptional regulation by CPC complex, to data. (A) Top row. Left, WT data. Middle, steady state solution of the SCM+ model, solved with parameter set P_{15348} . As the WER/MYB complex promotes GL2 expression [7–9], the total WER/MYB23 complex concentration, A_T , is used as a proxy for GL2. Right, model solution time course, stars on the horizontal axis show cortical cleft position. Bottom row shows *scm* mutant data and SCM- model results. SCM- model was also solved with parameter set P_{15348} . (B) Box plots showing the distributions of percentages of trichoblast and atrichoblast cells counted in H and N positions. The first boxplot on each graph shows the distribution of the data, Table 3. Each of the other boxplots contain results from twenty steady state solutions, each with a different random initial condition, for SCM+ and SCM- models, solved with parameter set shown.

The ten successful parameter sets did not occupy a common area of parameter space, nor were relationships found within those ten successful parameter sets which did not also hold for at least some of the 19,990 unsuccessful sets, S3 File. For all WER regulation models, solutions for parameter sets which failed could be; homogeneous, contain concentration differences which did not pass the 10% threshold (Section 2.2), have well defined cell types (Section 2.2) but trichoblast arrangement did not match the data in Table 3, or have poorly defined cell types, S3 File. Steady state solutions were found for all parameter sets tested, no oscillators were found.

Successful parameter sets were found for the model containing CPC complex regulation of *WER* and not for the models with CPC regulation of *WER* or no additional regulation of *WER*. These results suggest that a currently unknown *WER* transcriptional regulation is present in the root epidermis. Here, modelling has shown

that the unknown regulation could take the form of *WER* transcriptional repression by the CPC complex or a regulatory network component colocalised with the CPC complex.

3.2 Dysregulation of CPC movement in the SCM- regulatory network model is sufficient to reproduce *scm* mutant data.

For a parameter set to be labelled as a success, the parameter set must have reproduced *scm* mutant data when SCM was removed from the model (Section 2.2). SCM was previously hypothesised to be a cortical signal receptor because its removal from the plant decoupled trichoblasts from the cortical cleft [16]. With SCM's redefined role as a CPC importer [11], it was not clear that the dysregulation of CPC movement in *scm* mutant roots would be sufficient to reproduce *scm* mutant trichoblast, atrichoblast patterns. These modelling results show that it is indeed the case. The results show that trichoblast patterning can be decoupled from the cortical clefts without any change to the cortical signal or the cortical signal receptor, the decoupling is a result of CPC movement dysregulation alone, Figure 2.

3.3 SCM import of CPC reduces epidermal patterning sensitivity to reaction rate changes.

CPC is predominantly translated and transcribed in epidermal cells occupying N positions [14,15], where it competes with *WER* and *MYB23* to bind *GL3*, *EGL3*, thus preventing *WER/MYB23* complex formation [6,9]. SCM import of CPC, from cells in the N positions to cells in the H positions, likely aids patterning by reducing the amount of CPC available to compete with *WER* and *MYB23* for *GL3*, *EGL3*. If SCM import of CPC does aid patterning one might expect that models with SCM import of CPC would be less sensitive to parameter changes than models without SCM import of CPC. Sensitivity analysis was performed on the ten successful parameter sets found when *WER* transcription was repressed by cortical signal and the CPC complex, in both SCM+ and SCM- models (Section 2.3). In SCM+ models CPC movement is governed by diffusion plus SCM import, in the SCM- models CPC movement is governed by diffusion only, Equations (10) and (11). Insensitive regions were calculated (Section 2.3) for all core parameters, $P_{i,j}$, for SCM+ and SCM- models. Insensitive regions for SCM+ and SCM- models were then compared to understand if CPC import by SCM decreased the regulatory network's sensitivity to reaction rate changes.

To compare the sensitivity between SCM+ and SCM- models the difference between insensitive regions of the SCM- and SCM+ models was calculated for each core parameter $p_{i,j}$. The SCM- insensitive region was subtracted from the SCM+ sensitive region, for each core parameter, the resulting number defined how much less sensitive to changes in parameter $p_{i,j}$ the SCM+ model was when compared to the SCM- model. If the difference was negative the SCM+ model, containing CPC import and diffusion, was more sensitive to changes in parameter $p_{i,j}$ than the SCM- model, containing CPC diffusion only. Parameter sensitivity varied considerably between parameter sets, Figure 3A. For six of the ten parameter sets analysed, the SCM+ model was less sensitive than the SCM- model for all parameters, $p_{i,j}$. The other four parameter sets contained one, three or five, out of the thirty-eight, core parameters for which the SCM+ model was more sensitive than the SCM- model. Nonetheless, the total insensitive region for all ten parameter sets was greater for the SCM+ model than for the SCM- model, Figure 3B, indicating that SCM import of CPC increases the regulatory network's robustness against reaction rate changes.

3.4 Multiple binding site reactions within the MYB23 positive feedback loop are essential for successful root hair patterning.

Multiple binding sites have been reported for WER on the *MYB23* promotor [5], WER on the *CPC* promotor [14,15], and multiple GL3, EGL3, WER, MYB23 proteins are reported to be involved in WER/MYB23 complex formation [9]. Multiple binding sites at these three locations within the regulatory network, were incorporated into the model, Equations (6), (9) and (12) to (15). To investigate the contribution of each of the multiple binding site reactions to *Arabidopsis* root epidermal patterning, models containing the most up to date published reactions, i.e. SCM as a CPC importer and EGL3 restricted movement, Table 2, and each *WER* regulation mechanism, Tables 5 and 6, were solved with one, two and all three multiple binding site reactions removed, Table 7, for all 20,000 core parameter sets.

Table 7. Mechanistic parameter intervals for the multiple binding site investigation. Other parameter intervals are shown in Tables 1, 2 and 5. For one multiple binding site reaction removed, the name of the removed binding site reaction is shown. For two multiple binding site reactions removed, the name of the remaining binding site reaction is shown. n_1 and n_2 are parameters in the same multiple binding site reaction, WER/MYB23 complex formation.

	number of multiple binding site reactions removed	0	1			2			3
			multiple binding site removed			multiple binding site remaining			
		all	<i>CPC</i>	<i>MYB23</i>	<i>WER/MYB23</i> complex	<i>CPC</i>	<i>MYB23</i>	<i>WER/MYB23</i> complex	none
n_1	GL3, EGL3 in complex	{2,3,4}	{2,3,4}	{2,3,4}	1	1	1	{2,3,4}	1
n_2	WER, MYB23 in complex	{2,3,4}	{2,3,4}	{2,3,4}	1	1	1	{2,3,4}	1
n_3	<i>MYB23</i> translation	{2,3,4}	{2,3,4}	1	{2,3,4}	1	{2,3,4}	1	1
n_4	<i>CPC</i> translation	{2,3}	1	{2,3}	{2,3}	{2,3}	1	1	1

No successful parameter sets were found for models with any combination of multiple binding sites in which *WER* transcription was repressed by cortical signal alone, Table 8. For the models where *WER* transcription was repressed by cortical signal and CPC, three successful parameter sets were found for the model where multiple binding sites were on the *MYB23* promotor only. For all the three successful parameter sets, the number of WER binding sites on the *MYB23* promotor was $n_3 = 4$, the maximum value tested.

For models with *WER* transcriptional repression by cortical signal and CPC complex, successful parameter sets were found for numerous multiple binding site combinations. A notable result was that when one multiple binding site reaction was removed, the removal of multiple binding sites on the *MYB23* promotor was the only single multiple binding site removal which resulted in fewer successful parameter sets, when compared to the model with all multiple binding site reactions. Furthermore, when only one multiple binding site reaction remained, the *MYB23* promotor was the only multiple binding site reaction which, when alone, resulted in more successful parameter sets being found, compared to the model with all multiple binding site reactions, Table 8, Figure 4A. Taken together, these results suggested that the multiple binding site reaction on the *MYB23* promotor is a key driver of *Arabidopsis* root hair patterning.

Table 8. Numbers of successful parameter sets found in the multiple binding site investigation. Deep blue shaded cell shows the ten successful parameter sets found for the model with *WER* transcriptional repression by the cortical signal and CPC complex. The removal of multiple binding sites on the *MYB23* promotor reduced the number of successful parameter sets found (red shaded cell compared to deep blue cell). Multiple binding sites on the *MYB23* promotor only increased the number of successful parameter sets found (green shaded cells compared to blue cells). All successful parameter set numbers can be found in S4 File.

number of multiple binding site reactions removed	0	1			2			3
		multiple binding site removed			multiple binding site remaining			
<i>WER</i> transcriptional repression	all	<i>CPC</i>	<i>MYB23</i>	<i>WER/MYB23</i> <i>complex</i>	<i>CPC</i>	<i>MYB23</i>	<i>WER/MYB23</i> <i>complex</i>	none
cortical signal only	0	0	0	0	0	0	0	0
cortical signal and CPC	0	0	0	0	0	3	0	0
cortical signal and CPC complex	10	11	4	12	0	14	8	0

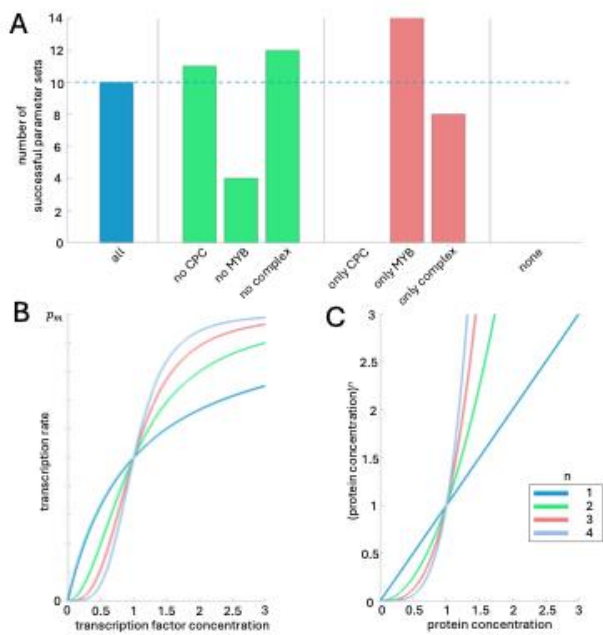


Figure 4: Cooperativity and oligomerisation. (A) The number of successful parameter sets found for model with *WER* transcription repressed by cortical signal and the CPC complex, for combinations of multiple binding site reactions (Table 7). The blue bar shows the data when all three multiple binding sites are present, green bars show the data when only one multiple binding site reaction is removed, and red bars show the data when only one multiple binding site reaction remains. The dotted line is for comparison between the data for all three multiple binding sites and fewer than three multiple binding sites. (B) Relationship between transcription rate and transcription factor concentration when transcription cooperativity is present within a promotor. Formula, $p_m[TF]^n(1 + [TF]^n)^{-1}$, where p_m is the maximum transcription rate, $[TF]$ is transcription factor concentration, and $n = \{1,2,3,4\}$ is cooperativity. (C) A graph showing the relationship between the rate of protein complex formation and the concentration of protein. $n = \{1,2,3,4\}$ is number of proteins in the complex.

No successful parameter sets were found when all multiple binding site reactions were removed, nor when only multiple binding sites on the *CPC* promotor remained. Successful parameter sets were found when multiple binding sites were only enabled on the *MYB23* promotor, Table 8, or *WER*/*MYB* complex formation reactions. *MYB23* transcription is part of a positive feedback loop with the *WER*/*MYB23* complex, such that the *WER*/*MYB23* complex promotes *MYB23* transcription, the translated *MYB23* can then bind *GL3/EGL3* to form the *WER*/*MYB23* complex, the *WER*/*MYB23* complex promotes *MYB23* transcription, and so on, Figure 1B. Thus, a single multiple binding site reaction within the *MYB23* positive feedback loop was sufficient to enable successful patterning.

Having more than one binding site on the modelled *MYB23* promotor, $n_3 \in \{2,3,4\}$, represents cooperativity between binding sites during transcriptional regulation. $n_1 \in \{2,3,4\}$, $n_2 \in \{2,3,4\}$ represents oligomerisation in the *WER*/*MYB23* complex. Mathematically, increasing cooperativity or the number of proteins within a complex, results in more pronounced nonlinearities, Figures 4B and 4C. Reactions with nonlinear dynamics can provide a patterning system with robustness against noise [31,32] and ultrasensitivity, depending largely on the value of n_i . For $n_i > 1$, a nonlinear reaction has a rate close to zero for small concentrations of regulatory proteins, rendering the reaction insensitive during periods when the regulatory protein concentrations are low. The insensitivity interval increases with n_i , Figures 4B and 4C. For larger values of n_i nonlinear reactions take on an ultrasensitive, switch like, behaviour, the insensitivity region is followed by a dramatic increase in the reaction rate. Reaction insensitivity at low regulatory protein concentrations could be developmentally advantageous. Noise has a greater impact on the relative concentrations of regulatory proteins when regulatory protein concentrations are low. Thus, reaction insensitivity at low regulatory protein concentrations would help to prevent noise from driving developmental patterning.

The *WER*/*MYB23* complex is the central transcription factor complex controlling the concentrations of numerous regulatory network components during *Arabidopsis* root epidermal cell differentiation and thus root hair patterning. These modelling results suggest that multiple binding sites in reactions within the *MYB23* positive feedback loop, particularly on *MYB23* translational regulation, are essential for correct root hair patterning. Their role may be two-fold, to protect the regulatory network from noise driven patterning early in development, and to create switch like dynamics when regulator concentrations pass some threshold.

3.5 Restricted *EGL3* movement and *CPC*/*EGL3* *WER*/*GL3* preferential binding enable epidermal patterning.

EGL3 movement has been reported to be restricted when compared to the movement of *GL3* [19]. In the models presented thus far, *EGL3* has been unable to move between epidermal cells, $D_E = 0$. To understand

if EGL3 restricted movement was necessary the models were solved with $D_E > 0$, Table 2, and each *WER* regulation mechanism, Tables 5 and 6, for all 20,000 core parameter sets. No successful parameter sets were found with $D_E > 0$, for models when *WER* transcription was repressed by cortical signal alone, or cortical signal plus CPC. Two successful parameter sets were found for *WER* transcription repressed by cortical signal and the CPC complex. One of the two successful core parameter sets for $D_G > 0$ was also one of the ten successful parameter sets found when $D_G = 0$, core parameter set $P_i = P_{4209}$, the other was core parameter set $P_i = P_{16189}$.

The diffusion coefficients of GL3 and EGL3 were compared for the two successful $D_G > 0$ parameter sets, P_{4209} and P_{16189} . For both parameter sets, the diffusion coefficient of GL3 was greater than the diffusion coefficient of EGL3, Table 9, suggesting that, for successful *Arabidopsis* root epidermal patterning, EGL3 movement must be restricted compared to GL3 movement. To further test if EGL3 movement must be restricted compared to GL3 movement for successful patterning, the ten successful parameter sets found with $D_E = 0$, plus the extra parameter set found for $D_G > 0$, were solved with $D_E = D_G$, all failed to reproduce experimental data, Table 3. Next the eleven parameter sets were solved with $D_E = 10^{-\alpha} D_G$, where $\alpha = \{0.05, 0.1, 0.15, \dots, 3\}$ to find the maximum value of D_E which will enable patterning. The largest value of D_E found to pattern successfully was denoted $D_{E_{MAX}}$, Table 9. All maximum successful EGL3 diffusion coefficients, $D_{E_{MAX}}$, were less than the GL3 diffusion coefficient. The data suggests that EGL3 movement must be restricted compared to GL3 movement, for successful *Arabidopsis* root epidermal patterning.

Table 9. GL3 and EGL3 diffusion coefficients. GL3 diffusion coefficient, D_G , EGL3 diffusion coefficient, D_E , and the maximum EGL3 diffusion coefficient tested which enables successful patterning, $D_{E_{MAX}}$, for each parameter set, i , in the investigation.

i	4209	16189	i	3423	3905	4209	4634	6365	10330	15122	15348	16189	18537	18878
D_G	5.86	7.53	D_G	1.04	6.09	5.86	3.15	4.53	8.91	6.78	5.14	7.53	0.15	4.44
D_E	0.52	3.68	$D_{E_{MAX}}$	0.92	0.48	0.66	0.63	0	1.41	0.06	0.13	3.77	0.14	0.99
			α	0.05	1.1	0.95	0.7	> 3	0.8	2.05	1.6	0.3	0.05	0.65

Both GL3 and EGL3 are translated and transcribed in trichoblast cells. The CPC concentration is greatest in trichoblast cells [17], which, in the model solutions, is due to the CPC complex dominating in these cells. The ability of GL3 to move more quickly from trichoblast to atrichoblast would be of limited use if the binding affinity between GL3 and CPC was greater than the binding affinity between EGL3 and CPC, as GL3 would become bound to CPC in trichoblast cells and become unable to move. Furthermore, once in the atrichoblast cell, if the GL3 CPC binding affinity was greater than the GL3 *WER*/MYB23 binding affinities then CPC would become bound to GL3 and trapped in the atrichoblast cells. It was thus hypothesised that CPC would bind EGL3 more strongly than GL3, and *WER*/MYB23 would bind GL3 more strongly than EGL3. Binding affinity relationships were calculated for each successful parameter set, with $D_E \geq 0$, Table 10, forst three data couumns. It was found that eight out of eleven parameter sets, $\approx 73\%$, supported the hypothesis that CPC bound EGL3 more strongly than GL3. Seven out of eleven parameter sets, $\approx 64\%$, supported the hypothesis that *WER* bound GL3 more strongly than EGL3. However, only four parameter sets, $\approx 36\%$, satisfied the relationship that MYB23 bound GL3 more strongly than EGL3, suggesting that preferential binding of MYB23 with GL3 is less important than *WER* preferentially binding GL3. This is because during early development the *WER* complex dominates over the MYB23 complex in atrichoblast cells. The *MYB23* promotor contains multiple *WER* binding sites [5] which means that the *WER* complex must become somewhat established before MYB23 is transcribed Figure 4B. Once MYB23 starts to be translated, the MYB23 positive feedback loop dominates in atrichoblast cells increasing the concentration of MYB23 such that the abundance alone is enough to sequester the majority GL3, enabling CPC to be imported into trichoblast cells.

Table 10. Binding affinity ratios and the dominating complex in trichoblast and atrichoblast cells. Data in the first three columns shows WER/GL3, MYB23/GL3 and CPC/GL3 binding affinity divided with WER/EGL3, MYB23/EGL3 and CPC/EGL3 binding affinity. If the ratio is less than 1 then the protein, WER, MYB23 or CPC, binds GL3 more strongly than EGL3, if the ratio is greater than 1 then the protein binds EGL3 more strongly than GL3. The complex which dominates in trichoblast and atrichoblast cells is also shown. Cells containing data that satisfies the relationships hypothesised as being optimal for epidermal patterning have been shaded in green.

<i>i</i>	WER	MYB23	CPC	dominating complex	
	$\frac{k_{12}k_{13}}{k_{11}k_{14}}$	$\frac{k_{16}k_{17}}{k_{15}k_{18}}$	$\frac{k_{22}k_{23}}{k_{21}k_{24}}$	trichoblast	atrichoblast
3423	0.40	0.02	37.78	CPC/EGL3	MYB23/GL3
3905	0.50	1.10	61.37	CPC/EGL3	MYB23/GL3
4209	0.04	2.04	1.07	CPC/GL3	MYB23/GL3
4634	5.48	1.47	0.44	CPC/GL3	MYB23/GL3
6365	4.72	11.01	0.49	CPC/GL3	MYB23/GL3
10330	0.06	1.95	1.72	CPC/EGL3	MYB23/GL3
15122	1.46	2.64	9.47	CPC/EGL3	MYB23/EGL3
15348	0.41	382.31	2.81	CPC/EGL3	MYB23/GL3
16189	0.94	0.09	17.37	CPC/EGL3	MYB23/GL3
18537	1.08	0.45	4.39	CPC/EGL3	MYB23/GL3
18878	0.33	0.23	119.62	CPC/EGL3	MYB23/GL3

The GL3 and EGL3 diffusion coefficients and binding affinity ratio analysis suggested that the CPC/EGL3 complex should be the most abundant complex in the trichoblast cells, and WER/GL3 and MYB23/GL3 complexes should be the most abundant complexes in atrichoblast cells. For a parameter set to have been considered successful, the SCM+ and SCM- models were solved with twenty noisy initial conditions and the solutions of both models matched the biological data (Section 2.2). Thus, for each of the successful parameter sets, there were twenty SCM+ solutions and twenty SCM- solutions. The concentrations of complexes CPC/GL3, CPC/EGL3, WER/GL3, WER/EGL3, MYB23/GL3, MYB23/EGL3, for all 220 SCM+ steady state solutions were plotted, Figure 5A. It was the case that, when all solutions were considered together, CPC/EGL3 was more abundant than CPC/GL3 in trichoblast cells and WER/GL3, MYB23/GL3 were more abundant than WER/EGL3, MYB23/EGL3 in atrichoblast cells.

The dominant complex in trichoblast cells was CPC/EGL3 giving insight as to why the sensitivity analysis performed in Section 3.3, Figure 3C, found that the removal of SCM import of CPC increased the network's sensitivity to changes in reaction rates related to CPC/EGL3 complex concentrations and not reaction rates related to GL3/CPC complex concentrations. Unexpectedly, there was less WER complex than CPC complex found in atrichoblast cells, the dominant complex in atrichoblast cells was the MYB23/GL3 complex. This result shows that, while WER is important in initiating correct epidermal patterning, once the MYB23 positive feedback loop is activated WER becomes redundant, further illustrating the importance of multiple binding sites in the MYB23 positive feedback loop for correct epidermal patterning, Section 3.4.

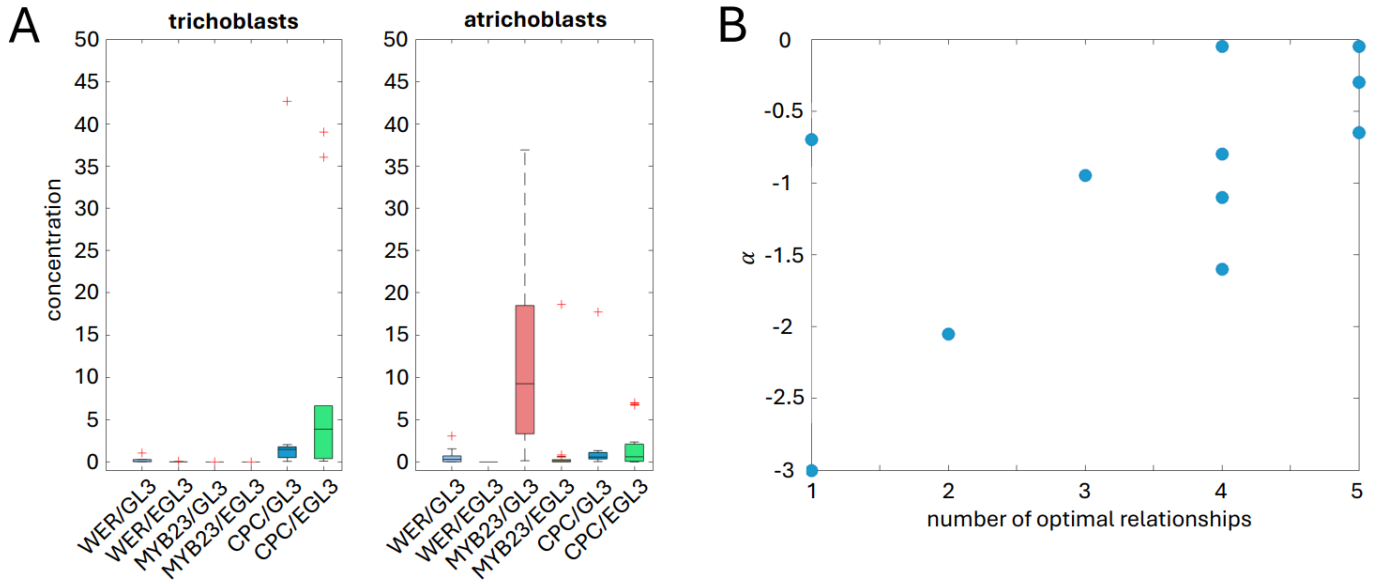


Figure 5: EGL3 movement. (A) Concentrations of protein complexes in trichoblast and atrichoblast cells, for all 220 SCM+ steady state solutions, with $D_E = D_{E_{MAX}}$, for the SCM+ model with *WER* translation regulated by the CPC complex and cortical signal. (B) Scatterplot showing the correlation between the number of optimal relationships a parameter set satisfied, Table 10, and the relationship between D_G and $D_{E_{MAX}}$. $D_{E_{MAX}} = 10^{-\alpha} D_G$, Table 9. One data point per parameter set.

The SCM+ complex concentrations for each of the eleven successful parameter sets were analysed individually, and the complex which dominated in the trichoblast and atrichoblast positions was recorded, Table 10, last two columns. It was found that for eight parameter sets, $\approx 73\%$, CPC/EGL3 was the dominating complex in trichoblast cells and for ten parameter sets, $\approx 91\%$, MYB23/GL3 was the dominating complex in atrichoblast cells. There were no successful parameter sets for which CPC/GL3 dominated in trichoblast cells and MYB23/EGL3 dominated in atrichoblast cells, demonstrating that at least one dominating complex had to be in the optimal form for successful epidermal patterning.

All the relationships hypothesised as being optimal for epidermal patterning were only satisfied by three parameter sets, $\approx 27\%$, and two parameter sets only satisfied one optimal relationship, $\approx 18\%$, Table 10. As there was no clear relationship between GL3 and maximum EGL3 diffusion coefficients, Table 9, it was asked if the order of magnitude difference between GL3 and EGL3 diffusion was correlated with the number of optimal relationships satisfied by each parameter set. The hypothesis was that the more optimal relationships a successful parameter set satisfied the closer to zero the value of $-\alpha$ would be, i.e. as more optimal relationships were satisfied the value of $D_{E_{MAX}}$ would approach D_G . Indeed, the number of optimal relationships satisfied was found to correlate with $-\alpha$, with a correlation coefficient of 0.67 which was calculated to be statistically significant with p-value 0.02, Figure 5B.

Collectively these data show that restricted movement of EGL3, compared to GL3, is essential for correct epidermal patterning. How much slower than GL3 movement, EGL3 movement must be, is dependent on other parameters within the regulatory network. If other parameters are set such that they aid the accumulation of CPC/EGL3 in trichoblast cells and WER/GL3, MYB23/GL3 in atrichoblast cells, then proper epidermal patterning is achieved with higher EGL3 diffusion coefficients.

4 Discussion.

The work presented here uses mathematical modelling to integrate a wealth of experimental data into one regulatory network model. The system under scrutiny was the regulatory network governing cell fate determination in the *Arabidopsis* root epidermis. The root epidermal cell fate network contains a central regulation complex whose regulation is determined by one positive feedback loop, two negative feedback loops, cell-cell signalling within the epidermal tissue, and positional cues from the underlying tissue.

A lot is known about components of the regulatory network, how they interact, and the effect of component removal on *Arabidopsis* root hair patterning. However, the complexity of the network has made it difficult to understand the contributions of individual components, and reactions, to the networks overall ability to control epidermal patterning.

The work here aimed to bridge that gap. The model was built to have a one-to-one relationship with the published regulatory network. Numerous mechanistic investigations were performed using the model. The investigations were designed to test; the sufficiency of our current knowledge to reproduce wild type and mutant data, the necessity for cooperativity and oligomerisation within reactions, reaction rate relationships, and the impact on patterning of cell-cell signalling properties.

4.1 Results summary.

Modelling results suggest that our current understanding of *WER* transcriptional regulation is incomplete. No successful parameter sets could be found for the model containing *WER* transcriptional regulation mechanisms supported by experimental data [12,9]. An obvious candidate for *WER* regulation would be for *WER* to promote its own transcription within atrichoblast cells, like *MYB23*, but this has already been shown not to be the case [12,5]. Thus, it was hypothesised that successful patterning may be achieved if *WER* transcription was repressed by a regulatory network component which dominates in trichoblast cells. As the CPC complex is a transcription factor complex which dominates in trichoblast cells, the CPC complex was chosen. The addition of *WER* transcriptional repression by the CPC complex enabled successful parameter sets to be found. *WER* regulation by the CPC complex was a hypothesised regulation, so all further mechanistic investigations were carried out in the models with published and hypothesised *WER* regulation. For all but one of the subsequent investigations, the model with *WER* regulation by the CPC complex was the only model for which successful parameter sets could be found.

In recent years the role of SCM has been revised. Initially SCM was hypothesised to be a cortical signal receptor because it's removal from the plant decoupled trichoblasts from the cortical cleft [16]. SCM has since been shown to function as a CPC importer [11]. It was easy to understand how the removal of a cortical signal receptor would decouple epidermal patterning from its positional cues. However, it was not obvious that the removal of CPC import from the regulatory network, while leaving cortical signal receptors and positional cues intact, could produce an epidermal pattern which appeared to be positional signalling impaired. Here, it was shown that the removal of CPC import from the regulatory network was sufficient to reproduce *scm* mutant data.

The import of CPC by SCM was shown to make the regulatory network's ability to reproduce biological data more robust against changes in reaction rates, when compared to the regulatory network with CPC movement governed by diffusion alone. These results confirm that the directed removal of CPC from N positioned cells is beneficial for the *WER*/*MYB23* complex to become the dominant complex in N positions, and for the CPC complex to dominate in H positions.

The *WER*/*MYB23* complex promotes the transcription of *CPC* and *MYB23* [14,15,5]. Multiple *WER* binding sites have been shown to exist on the *CPC* and *MYB23* promoters. The formation of the *WER*/*MYB23* complex also involves multiple binding site reactions and it is predicted that more than one of the *WER*, *MYB23*, *GL3* and *EGL3* proteins come together to form the complex [9]. The question of how multiple binding site reactions contributed to successful epidermal patterning was addressed. No benefit to successful patterning could be found for cooperativity on *CPC* transcriptional regulation. It was found that a multiple binding site reaction within the *MYB23* positive feedback loop was essential for the regulatory network to reproduce biological data, and that cooperativity on *MYB23* transcription contributed more to successful patterning than *WER*/*MYB23* complex oligomerisation. Cooperativity within transcription and oligomerisation result in reaction dynamics whereby reactions are insensitive for low concentrations of reactants and highly sensitive for reactant concentrations past some threshold. These results suggest that for the *Arabidopsis* root epidermis to pattern successfully the positive feedback loop which amplifies the concentration of the central regulatory complex, the *WER*/*MYB23* complex, must be protected against noise driven patterning early in development, and have switch like dynamics which enable *WER*/*MYB* complex domination when regulator concentrations pass some threshold.

GL3 and EGL3 are predominantly translated in trichoblast cells [6]. GL3 has been shown to move into atrichoblast cells, where it accumulates [13], whereas EGL3 remains in the trichoblast cells [19]. The necessity of GL3, EGL3 differential movement was investigated and found to be essential for the regulatory network model to reproduce data. It was found that the regulatory network could reproduce root hair patterning when EGL3 was able to diffuse between cells, however the diffusion coefficient of EGL3 had to be less than the diffusion coefficient of GL3, how much less depended on other parameters within the network. Parameter and steady state concentration relationships favourable for correct patterning were defined. Namely, CPC preferentially binds EGL3 during complex formation, WER and MYB23 preferentially bind GL3 during complex formation, CPC/GL3 is the dominant complex in trichoblast cells and MYB23/GL3 is the dominant complex in atrichoblast cells. The more favourable relationships satisfied, the smaller the difference between GL3 and EGL3 movement could be while still allowing the regulatory network to reproduce patterning data.

4.2 An integrated understanding.

The results of the work presented give an integrated understanding of how the components and reactions within the Arabidopsis root epidermal regulatory network come together to ensure robust root hair patterning. Identical epidermal cells emerge from the root apical meristem. The identical cells start to transcribe *WER*, *GL3* and *EGL3*. A positional cue reduces the transcription of *WER* in epidermal cells occupying the H positions, distinguishing H position and N position cells. Thus, cells in the N position start to translate more *WER* and form more *WER* complex than cells in the H positions. An abundance of *WER* complex in N position cells reduces *GL3* and *EGL3* transcription. For the *WER* complex to remain dominant in the N positions, *WER* must bind GL3 which has diffused into N position cells from the H positions. *EGL3* movement is restricted so the majority of *EGL3* remains in H position cells.

Cooperativity between *WER* binding sites on the *CPC* and *MYB23* promoters dictates that the *WER* complex concentration must build up before the *WER* complex starts to effectively promote *CPC* and *MYB23* translation. The initial insensitivity of the regulatory network to changes in *WER* complex concentration is essential to protect epidermal patterning from noise driven *WER* complex concentration changes early in development, when *WER* complex concentrations are low. Once *MYB23* transcription begins, the *MYB23* positive feedback loop is activated and *MYB23* complex concentrations increase dramatically. The abundance of *MYB23* in N position cells sequesters GL3, and any EGL3, to make the *MYB23* complex the dominant atrichoblast complex. *WER* becomes redundant after the initial developmental phase. Thus, the role of *WER* appears to be to receive positional cues during early development, with these positional cues transmitted through *WER* becoming ineffective later in development.

The promotion of *CPC* transcription by the *WER*/*MYB* complex leads to an abundance of *CPC* in N position cells. *CPC* can also form a complex with GL3 and EGL3 and thus competes with *WER* and *MYB* for GL3/EGL3 binding. To counteract the accumulation of *CPC* in the N positions, *CPC* is imported into H position cells from neighbouring N position cells. *CPC* has a stronger affinity to EGL3 than GL3. The preferential binding of EGL3 and *CPC* leaves GL3 unbound and free to diffuse from the H position cells into N position cells, where GL3 can be used to maintain high *WER*/*MYB* complex concentrations.

This work hypothesises that for the regulatory network to reproduce WT and *scm* mutant root epidermal patterning, the *CPC* complex, or other regulatory network component colocalised with the *CPC* complex, must inhibit *WER* translation to ensure that *WER* complex concentrations do not increase to levels which would enable it to initiate the *MYB23* positive feedback loop in all cells.

Acknowledgements.

Funded by the Leverhulme Project Grant RPG-2021-053.

References.

1. Dolan L, Duckett CM, Grierson C, Linstead P, Schneider K, Lawson E, Dean C, Poethig S, Roberts K. Clonal relationships and cell patterning in the root epidermis of *Arabidopsis*. *Development*. 1994 Sep 1;120(9):2465–74.
2. Galway ME, Masucci JD, Lloyd AM, Walbot V, Davis RW, Schiefelbein JW. The TTG Gene Is Required to Specify Epidermal Cell Fate and Cell Patterning in the *Arabidopsis* Root. *Dev Biol*. 1994 Dec 1;166(2):740–54.
3. Berger F, Haseloff J, Schiefelbein J, Dolan L. Positional information in root epidermis is defined during embryogenesis and acts in domains with strict boundaries. *Curr Biol*. 1998 Mar;8:421–30.
4. Lee MM, Schiefelbein J. WEREWOLF, a MYB-Related Protein in *Arabidopsis*, Is a Position-Dependent Regulator of Epidermal Cell Patterning. *Cell*. 1999 Nov;99(5):473–83.
5. Kang YH, Kirik V, Hulskamp M, Nam KH, Hagely K, Lee MM, Schiefelbein J. The *MYB23* Gene Provides a Positive Feedback Loop for Cell Fate Specification in the *Arabidopsis* Root Epidermis. *Plant Cell*. 2009 May 22;21(4):1080–94.
6. Bernhardt C, Lee MM, Gonzalez A, Zhang F, Lloyd A, Schiefelbein J. The bHLH genes *GLABRA3* (*GL3*) and *ENHANCER OF GLABRA3* (*EGL3*) specify epidermal cell fate in the *Arabidopsis* root. *Development*. 2003 Dec 29;130(26):6431–9.
7. Di Cristina M, Sessa G, Dolan L, Linstead P, Baima S, Ruberti I, Morelli G. The *Arabidopsis* Athb-10 (*GLABRA2*) is an HD-Zip protein required for regulation of root hair development. *Plant J*. 1996 Sep;10(3):393–402.
8. Masucci JD, Rerie WG, Foreman DR, Zhang M, Galway ME, Marks MD, Schiefelbein JW. The homeobox gene *GLABRA 2* is required for position-dependent cell differentiation in the root epidermis of *Arabidopsis thaliana*. *Development*. 1996 Apr 1;122(4):1253–60.
9. Song SK, Ryu KH, Kang YH, Song JH, Cho YH, Yoo SD, Schiefelbein J, Lee MM. Cell Fate in the *Arabidopsis* Root Epidermis Is Determined by Competition between WEREWOLF and CAPRICE. *Plant Physiol*. 2011 Nov 3;157(3):1196–208.
10. Kwak SH, Schiefelbein J. The role of the SCRAMBLED receptor-like kinase in patterning the *Arabidopsis* root epidermis. *Dev Biol*. 2007 Feb;302(1):118–31.
11. Song JH, Kwak SH, Nam KH, Schiefelbein J, Lee MM. QUIRKY regulates root epidermal cell patterning through stabilizing SCRAMBLED to control CAPRICE movement in *Arabidopsis*. *Nat Commun*. 2019 Apr 15;10(1):1744.
12. Savage NS, Walker T, Wieckowski Y, Schiefelbein J, Dolan L, Monk NAM. A Mutual Support Mechanism through Intercellular Movement of CAPRICE and *GLABRA3* Can Pattern the *Arabidopsis* Root Epidermis. Weigel D, editor. *PLoS Biol*. 2008 Sep 23;6(9):e235.
13. Bernhardt C, Zhao M, Gonzalez A, Lloyd A, Schiefelbein J. The bHLH genes *GL3* and *EGL3* participate in an intercellular regulatory circuit that controls cell patterning in the *Arabidopsis* root epidermis. *Development*. 2005 Jan 15;132(2):291–8.
14. Koshino-Kimura Y, Wada T, Tachibana T, Tsugeki R, Ishiguro S, Okada K. Regulation of CAPRICE Transcription by MYB Proteins for Root Epidermis Differentiation in *Arabidopsis*. *Plant Cell Physiol*. 2005 Jun 1;46(6):817–26.
15. Ryu KH, Kang YH, Park Y hwan, Hwang I, Schiefelbein J, Lee MM. The WEREWOLF MYB protein directly regulates *CAPRICE* transcription during cell fate specification in the *Arabidopsis* root epidermis. *Development*. 2005 Nov 1;132(21):4765–75.

16. Kwak SH, Shen R, Schiefelbein J. Positional Signaling Mediated by a Receptor-like Kinase in *Arabidopsis*. *Science*. 2005 Feb 18;307(5712):1111–3.
17. Kurata T, Ishida T, Kawabata-Awai C, Noguchi M, Hattori S, Sano R, Nagasaka R, Tominaga R, Koshino-Kimura Y, Kato T, Sato S, Tabata S, Okada K, Wada T. Cell-to-cell movement of the CAPRICE protein in *Arabidopsis* root epidermal cell differentiation.
18. Kwak SH, Schiefelbein J. A Feedback Mechanism Controlling SCRAMBLED Receptor Accumulation and Cell-Type Pattern in *Arabidopsis*. *Curr Biol*. 2008 Dec;18(24):1949–54.
19. Kang YH, Song SK, Schiefelbein J, Lee MM. Nuclear Trapping Controls the Position-Dependent Localization of CAPRICE in the Root Epidermis of *Arabidopsis*. *Plant Physiol*. 2013 Sep;163(1):193–204.
20. Benítez M, Espinosa-Soto C, Padilla-Longoria P, Alvarez-Buylla ER. Interlinked nonlinear subnetworks underlie the formation of robust cellular patterns in *Arabidopsis* epidermis: a dynamic spatial model. *BMC Syst Biol*. 2008 Dec;2(1):98.
21. Hill AV. The combinations of haemoglobin with oxygen and with carbon monoxide. *Proc Physiol*. 1910 Jan 22;40:iv–vii.
22. Weiss JN. The Hill equation revisited: uses and misuses. *FASEB J*. 1997 Sep;11(11):835–41.
23. Song et al. - 2011 - Cell Fate in the *Arabidopsis* Root Epidermis Is Det.pdf.
24. Kwak SH, Woo S, Lee MM, Schiefelbein J. Distinct Signaling Mechanisms in Multiple Developmental Pathways by the SCRAMBLED Receptor of *Arabidopsis*. *PLANT Physiol*. 2014 Oct 1;166(2):976–87.
25. Chaudhary A, Chen X, Leśniewska B, Boikine R, Gao J, Wolf S, Schneitz K. Cell wall damage attenuates root hair patterning and tissue morphogenesis mediated by the receptor kinase STRUBBELIG. *Development*. 2021 Jul 15;148(14):dev199425.
26. Lampropoulos A, Sutikovic Z, Wenzl C, Maegele I, Lohmann JU, Forner J. GreenGate - A Novel, Versatile, and Efficient Cloning System for Plant Transgenesis. Janssen PJ, editor. *PLoS ONE*. 2013 Dec 20;8(12):e83043.
27. Kümpers BMC, Han J, Vaughan-Hirsch J, Redman N, Ware A, Atkinson JA, Leftley N, Janes G, Castiglione G, Tarr PT, Pyke K, Voß U, Wells DM, Bishopp A. Dual expression and anatomy lines allow simultaneous visualization of gene expression and anatomy. *Plant Physiol*. 2022 Jan 20;188(1):56–69.
28. Zhang X, Henriques R, Lin SS, Niu QW, Chua NH. *Agrobacterium*-mediated transformation of *Arabidopsis thaliana* using the floral dip method. *Nat Protoc*. 2006 Aug;1(2):641–6.
29. Kurihara D, Mizuta Y, Sato Y, Higashiyama T. ClearSee: a rapid optical clearing reagent for whole-plant fluorescence imaging. *Development*. 2015 Jan 1;dev.127613.
30. Ursache R, Andersen TG, Marhavý P, Geldner N. A protocol for combining fluorescent proteins with histological stains for diverse cell wall components. *Plant J*. 2018 Jan;93(2):399–412.
31. Green RM, Fish JL, Young NM, Smith FJ, Roberts B, Dolan K, Choi I, Leach CL, Gordon P, Cheverud JM, Roseman CC, Williams TJ, Marcucio RS, Hallgrímsson B. Developmental nonlinearity drives phenotypic robustness. *Nat Commun*. 2017 Dec 6;8(1):1970.
32. Steinacher A, Bates DG, Akman OE, Soyer OS. Nonlinear Dynamics in Gene Regulation Promote Robustness and Evolvability of Gene Expression Levels. Proulx SR, editor. *PLOS ONE*. 2016 Apr 15;11(4):e0153295.

S1 File

Supporting information for Section 2.2, Table 3, of main manuscript. WT and *scm* mutant image analysis available on GitHub [ref](#).

Table S1-1. Wildtype data calculated from GL2mT images.

root	H		N	
	H	N	H	N
1	87.5	12.5	0.0	100.0
2	100.0	0.0	0.0	100.0
3	100.0	0.0	0.0	100.0
4	100.0	0.0	0.0	100.0
5	100.0	0.0	0.0	100.0
6	87.5	12.5	0.0	100.0
7	85.7	14.3	0.0	100.0
8	75.0	25.0	9.1	90.9
9	87.5	12.5	8.3	91.7
10	100.0	0.0	0.0	100.0
11	100.0	0.0	8.3	91.7
12	100.0	0.0	0.0	100.0
13	100.0	0.0	0.0	100.0
14	100.0	0.0	0.0	100.0
15	87.5	12.5	0.0	100.0
16	75.0	25.0	0.0	100.0
17	100.0	0.0	0.0	100.0
18	88.9	11.1	0.0	100.0
19	100.0	0.0	0.0	100.0
20	100.0	0.0	0.0	100.0
21	100.0	0.0	0.0	100.0
22	87.5	12.5	0.0	100.0
mean	93.7	6.3	1.2	98.8
standard deviation	8.4	8.4	3.0	3.0

Table S1-2. *scm* mutant data calculated from eleven figures within six publications [1–6].

reference	figure	mutant	marker	H		N	
				H	N	H	N
Kwak 2005 [1]	1A	scm-1	GL2	66.7	33.3	23.6	76.4
Kwak 2005 [1]	1E	scm-2	GL2	54.5	45.5	36.0	64.0
Kwak 2005 [1]	2A	scm-2	CPC	57.1	42.9	15.0	85.0
Kwak 2005 [1]	2B	scm-2	WER	85.7	14.3	7.7	92.3
Kwak 2005 [1]	2D	scm-2	EGL3	72.5	27.5	11.3	88.7
Kwak 2007 [2]	2A	scm-2	GL2	47.6	52.4	13.0	87.0
Kwak 2007 [2]	7B	scm-2	GL2	39.3	60.7	40.0	60.0
Song 2011 [3]	2B	scm-2	GL2	66.7	33.3	6.3	93.7
Kwak 2014 [4]	2B	scm-2	GL2	55.6	44.4	37.0	63.0
Song 2019 [5]	2b	scm-2	GL2	72.4	27.6	48.3	51.7
Chaudhary 2021 [6]	3J	sub-9	GL2	61.5	38.5	8.7	91.3
mean				61.8	38.2	22.4	77.6
standard deviation				12.9	12.9	15.2	15.2

References.

1. Kwak SH, Shen R, Schiefelbein J. Positional Signaling Mediated by a Receptor-like Kinase in *Arabidopsis*. *Science*. 2005 Feb 18;307(5712):1111–3.
2. Kwak SH, Schiefelbein J. The role of the SCRAMBLED receptor-like kinase in patterning the Arabidopsis root epidermis. *Developmental Biology*. 2007 Feb;302(1):118–31.
3. Song SK, Ryu KH, Kang YH, Song JH, Cho YH, Yoo SD, Schiefelbein J, Lee MM. Cell Fate in the Arabidopsis Root Epidermis Is Determined by Competition between WEREWOLF and CAPRICE. *Plant Physiology*. 2011 Nov 3;157(3):1196–208.
4. Kwak SH, Woo S, Lee MM, Schiefelbein J. Distinct Signaling Mechanisms in Multiple Developmental Pathways by the SCRAMBLED Receptor of Arabidopsis. *PLANT PHYSIOLOGY*. 2014 Oct 1;166(2):976–87.
5. Song JH, Kwak SH, Nam KH, Schiefelbein J, Lee MM. QUIRKY regulates root epidermal cell patterning through stabilizing SCRAMBLED to control CAPRICE movement in Arabidopsis. *Nat Commun*. 2019 Apr 15;10(1):1744.
6. Chaudhary A, Chen X, Leśniewska B, Boikine R, Gao J, Wolf S, Schneitz K. Cell wall damage attenuates root hair patterning and tissue morphogenesis mediated by the receptor kinase STRUBBELIG. *Development*. 2021 Jul 15;148(14):dev199425.

S2 File

Supporting information for Section 2.4 of main manuscript.

Table S2. Primers used for cloning fragments for the GLABRA2 genomic fragment and Gly-Ser linker-mTurquoise fusion protein. Primers are expressed as 5'-3' orientation.

Primer name	Primer sequence
GL2 B Fwd 1	aacaggtctcaACAATGAAGTCGATCGATGGCTG
GL2 B Fwd 2	aacaggtctcaGGTATCCGTGGAGGACAG
GL2 B Rev 1	aacaggtctcaTACCGAGACGTCCACTATTG
GL2 B Rev 2	aacaggtctcaAGCCGCAATCTTCGATTTGTAGAC
Linker-mTurq C Fwd	aacaggtctcaGGCTtccggaggtggtggttctggtGGGGGTGGCTCTgtgagcaagggcgaggag
mTurq C Rev	aacaggtctcaCTGAttactcttcttcttgatcagcttctgtg

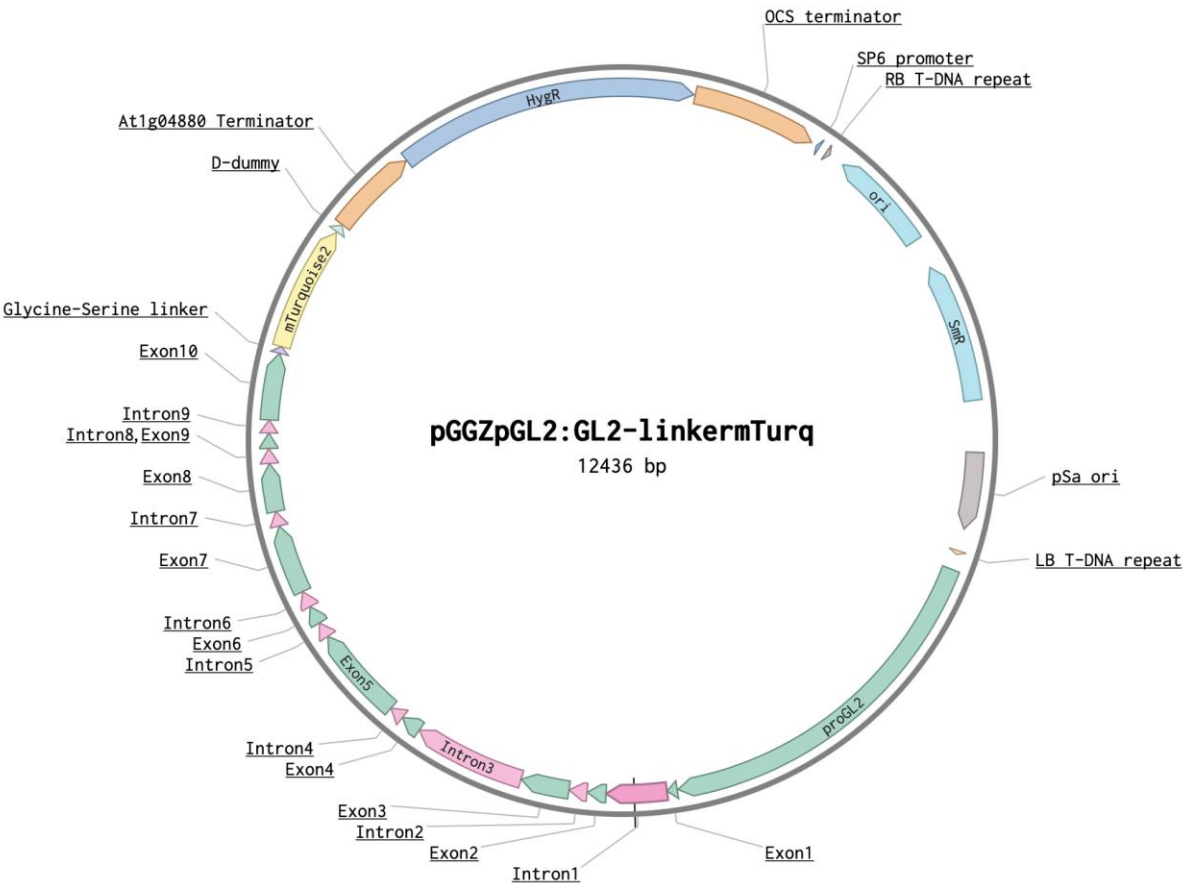


Figure S2. Plasmid map of GL2-mTurquoise reporter construct as sequenced. Total size of plasmid 12436 base pairs.

Acknowledgement. The Salk Institute Genomic Analysis Laboratory provided the sequence-indexed Arabidopsis T-DNA insertion mutants.

S3 File

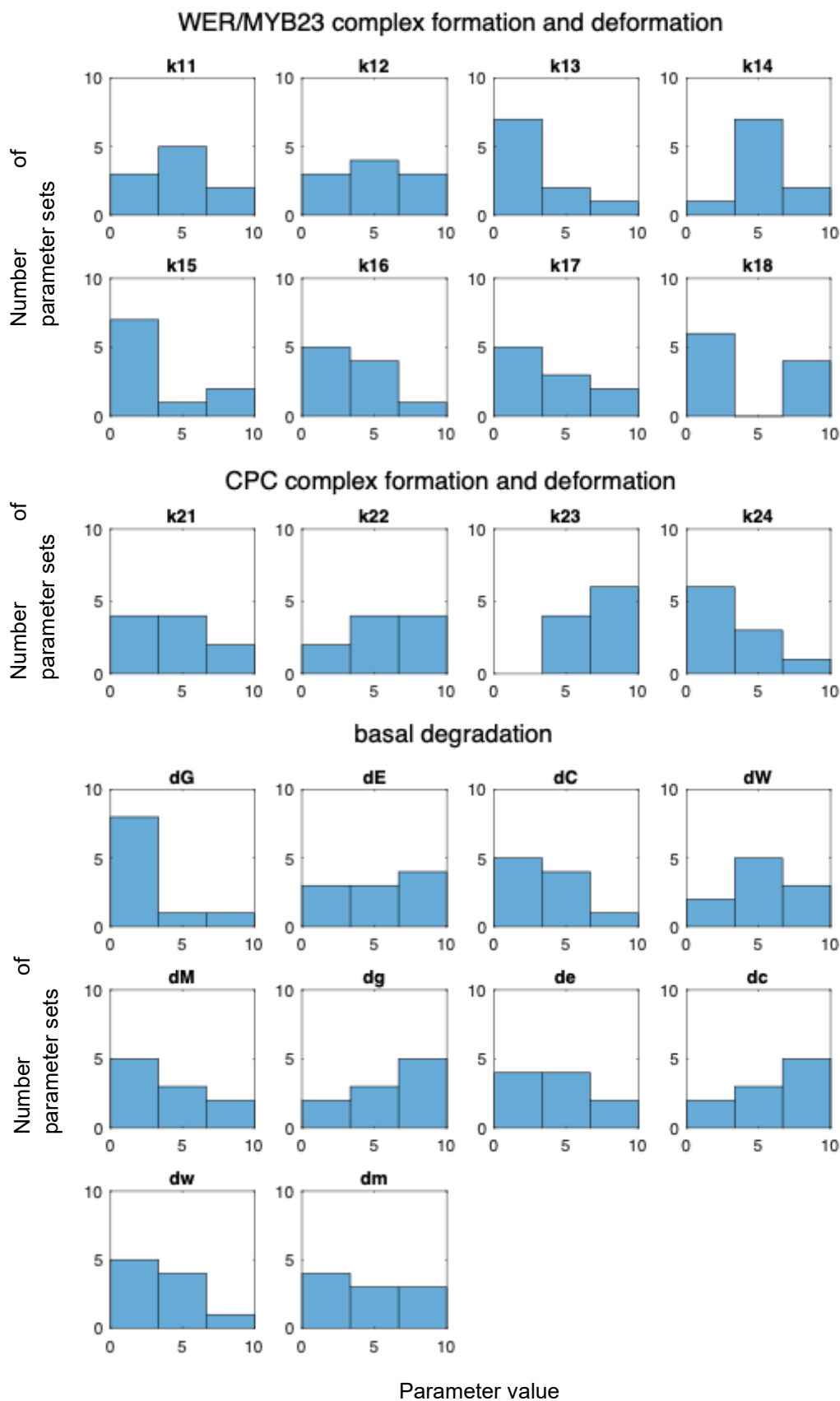
Supporting information for Section 3.1 of main manuscript.

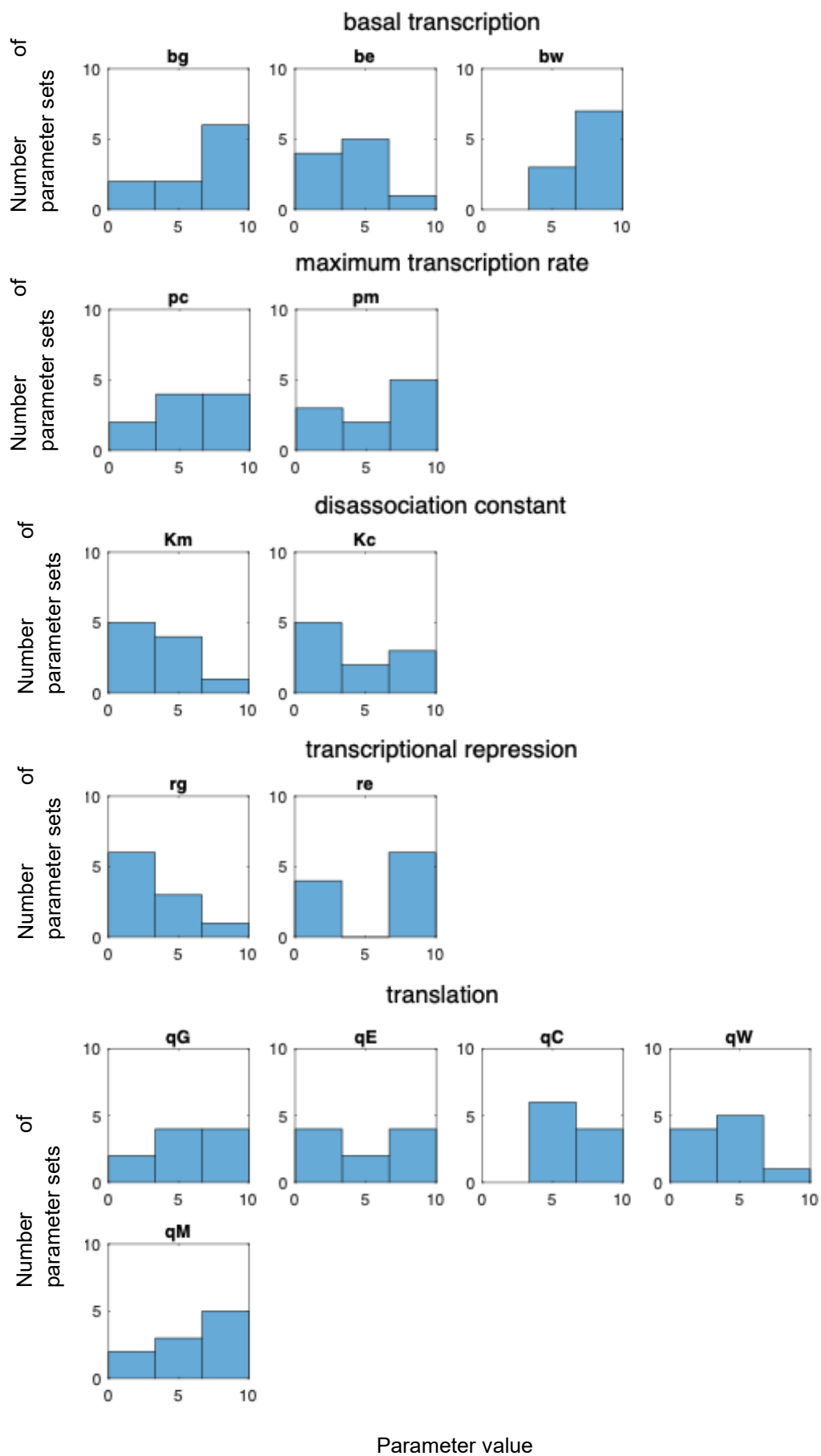
Table S3-1. Parameter values for the 10 successful parameter sets, given to two significant figures.

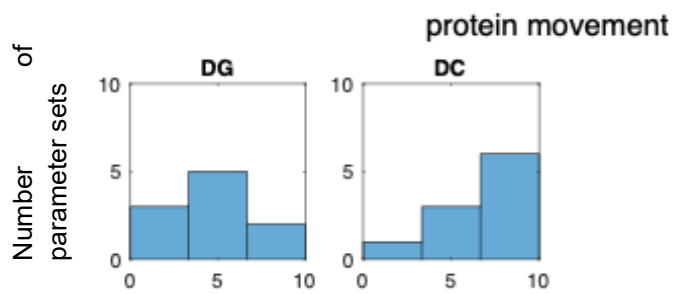
	parameter set number	3423	3905	4209	4634	6365	10330	15122	15348	18537	18878
k_{11}	A_{GW} association	5.95	4.92	4.61	0.82	0.28	7.36	3.38	8.57	2.07	5.66
k_{12}	A_{GW} disassociation	1.67	4.80	0.46	6.79	4.14	9.09	2.82	8.85	5.96	5.47
k_{13}	A_{EW} association	5.29	2.31	2.34	3.18	1.10	0.17	8.71	1.48	3.19	3.40
k_{14}	A_{EW} disassociation	3.66	4.52	6.31	4.80	3.46	3.30	4.97	3.74	8.53	9.89
k_{15}	A_{GM} association	1.50	2.28	0.42	4.03	0.93	2.46	7.57	0.26	2.59	7.55
k_{16}	A_{GM} disassociation	0.09	6.54	0.81	1.74	2.63	5.71	3.54	5.02	9.59	1.63
k_{17}	A_{EM} association	2.00	3.27	3.25	4.09	3.48	5.87	9.13	7.46	1.01	1.83
k_{18}	A_{EM} disassociation	7.63	8.51	3.13	1.20	0.90	7.00	1.61	0.38	8.33	1.69
k_{21}	I_{GC} association	2.68	1.23	9.23	6.53	9.73	5.55	5.82	4.63	2.66	0.60
k_{22}	I_{GC} disassociation	6.21	7.82	8.67	2.07	6.32	4.23	7.03	3.94	7.27	1.98
k_{23}	I_{EC} association	9.98	9.62	6.51	5.66	6.28	6.94	9.18	7.77	6.64	7.58
k_{24}	I_{EC} disassociation	0.61	1.00	5.74	4.09	8.26	3.07	1.17	2.36	4.13	0.21
d_G	GL3 protein	0.60	1.17	1.07	2.25	1.78	4.40	9.54	2.97	3.18	1.97
d_E	EGL3 protein	2.38	3.34	6.72	5.98	6.99	9.55	1.82	6.70	3.18	6.12
d_C	CPC protein	3.30	1.74	0.99	5.46	1.46	3.23	4.44	7.71	3.84	4.86
d_W	WER protein	9.57	6.03	1.06	5.43	5.71	5.82	9.20	3.83	1.74	6.71
d_M	MYB23 protein	6.54	8.03	1.76	0.84	4.67	1.16	1.93	9.98	2.85	4.78
d_g	GL3 mRNA	8.17	3.94	2.41	7.09	6	9.18	7.17	4.23	8.93	0.82
d_e	EGL3 mRNA	2.55	1.45	6.51	5.16	8.53	3.03	5.18	0.60	7.13	6.61
d_c	CPC mRNA	7.45	6.77	3.32	7.81	8.76	3.33	4.71	6.73	3.89	3.99
d_w	WER mRNA	8.47	5.97	3.25	1.20	3.29	0.43	0.95	4.51	4.77	5.91
d_m	MYB23 mRNA	1.68	6.07	7.58	4.15	1.50	1.77	8.87	0.40	6.83	3.63
b_g	GL3 mRNA	8.27	5.41	8.37	8.02	4.61	7.66	7.40	1.80	9.23	0.68
b_e	EGL3 mRNA	6.36	1.07	4.53	6.44	9.98	2.45	3.90	1.86	4.60	2.61
b_w	WER mRNA	6.90	9.75	4.39	7.48	6.10	6.75	7.01	4.52	8.21	8.62
p_c	CPC mRNA	5.64	6.01	8.22	4.20	1.73	1.15	9.99	6.36	8.78	7.80
p_m	MYB23 mRNA	9.91	9.99	4.92	8.19	1.97	1.41	9.20	5.71	8.39	2.19
K_c	WER on CPC transcript	1.53	9.41	2.03	5.07	2.54	3.63	6.23	6.33	2.56	1.97
K_m	WER on MYB23 transcript	2.66	2.95	1.27	5.93	4.18	9.25	7.02	9.13	3.27	3.24
r_g	GL3 by WER/MYB23 complex	2.80	5.04	6.89	0.80	4.29	5.57	1.08	0.85	0.32	0.47
r_e	EGL3 by WER/MYB23 complex	2.76	7.08	1.43	2.94	8.88	3.33	6.87	9.57	8.30	9.74
q_G	GL3 protein	3.90	5.83	2.38	3.53	8.48	5.29	0.59	9.26	7.07	6.76
q_E	EGL3 protein	0.52	1.66	1.92	1.65	3.90	9.54	6.98	5.01	7.50	9.77
q_C	CPC protein	4.25	9.22	6.11	3.77	5.40	8.54	5.55	7.24	5.60	8.92
q_W	WER protein	1.63	2.42	4.91	3.17	4.29	3.80	9.42	4.82	0.98	4.40
q_M	MYB23 protein	0.29	6.08	6.53	1.30	8.25	7.56	8.34	7.57	5.30	7.37
D_G	GL3 diffusion	1.04	6.09	5.86	3.15	4.53	8.91	6.78	5.14	0.15	4.44
D_C	CPC diffusion	6.71	5.64	7.77	9.14	9.21	6.27	5.68	7.14	9.13	1.40
n_1	GL3, EGL3	2	4	3	3	2	4	2	3	2	3
n_2	WER, MYB23	2	2	3	3	2	3	3	3	2	2
n_3	WER on MYB23	4	3	2	4	2	3	2	3	4	3

n_4	WER on <i>CPC</i>	3	3	3	2	2	2	2	3	3	3
r_{w11}	by <i>CPC</i>	0	0	0	0	0	0	0	0	0	0
r_{w12}	by <i>CPC</i> complex	7.94	9.44	8.96	9.93	0.13	3.71	6.34	3.58	2.46	7.17
D_E	diffusion	0	0	0	0	0	0	0	0	0	0
S	SCM+	1	1	1	1	1	1	1	1	1	1
S	SCM-	0	0	0	0	0	0	0	0	0	0
\tilde{D}_C	<i>CPC</i> import via SCM	3.01	7.50	9.90	3.06	8.07	1.99	4.81	4.33	0.04	6.64
R_X	unknown receptor	0.25	1.6e-2	7.8e-3	7.8e-3	3.1e-2	5.0e-4	0.25	1.6e-2	3.1e-2	0.25
r_{w21}	<i>WER</i> repression via R_X	5.37	3.50	6.87	3.67	7.96	1.46	4.58	8.13	7.84	7.48
C_{0max}	maximum of random initial conditions interval	0.5	6.3e-2	6.3e-2	0.13	0.50	6.3e-2	0.50	0.50	0.50	0.50

Fig S3-1. Histograms of the parameter values of the 10 successful parameter sets. Distribution of parameter values for the 10 successful parameter sets. Distributions for the unsuccessful parameter sets were uniform for all parameters.







Parameters changed during mechanistic investigations
(parameters rw11, DE, and S are set to 0 in these models)

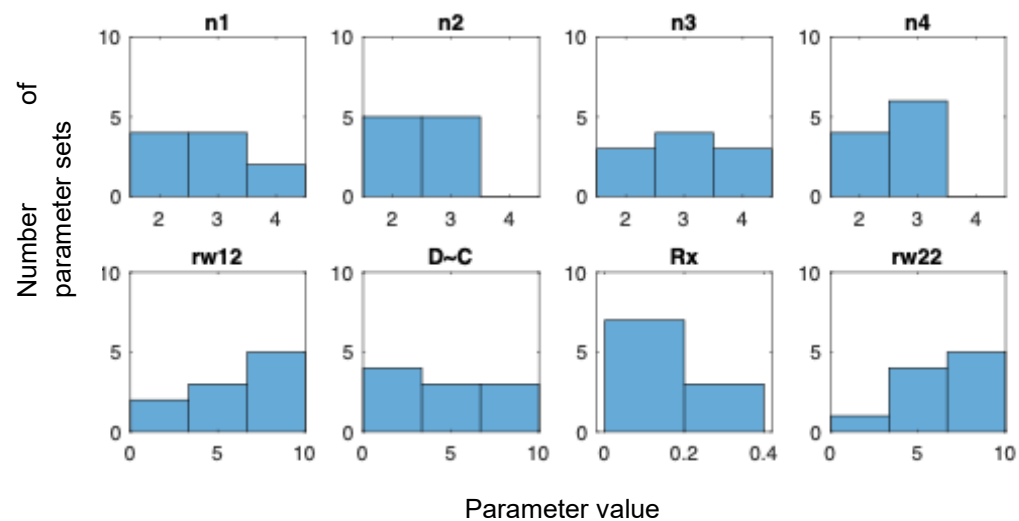
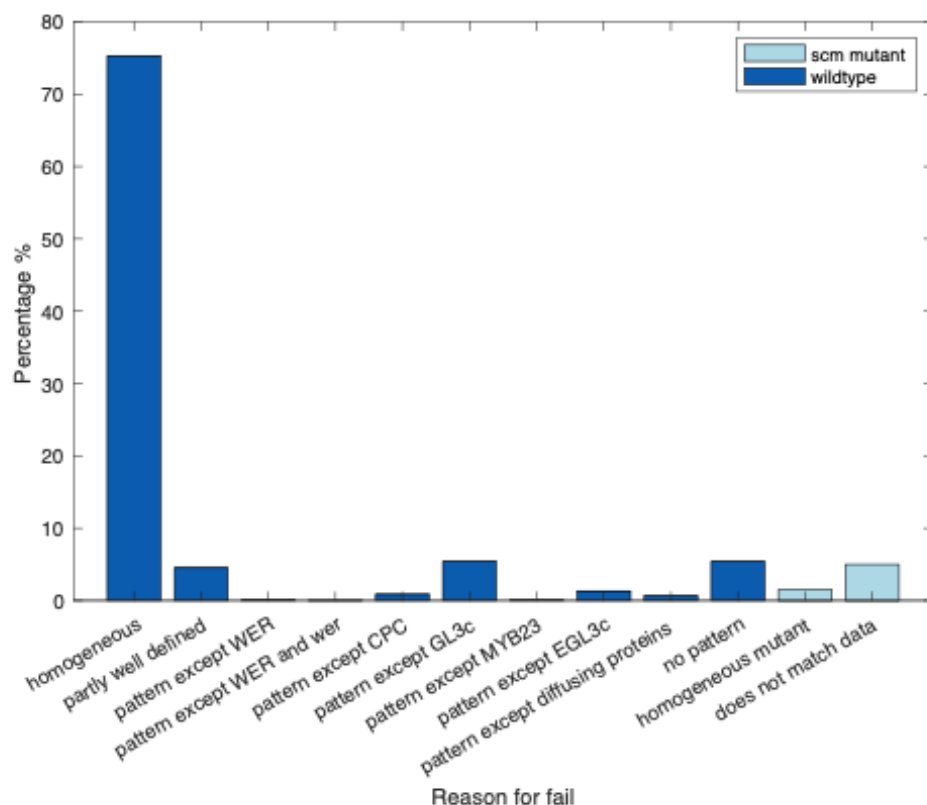


Table S3-2. Breakdown of the reasons for failure of the unsuccessful parameter sets.

	fail description	number of parameter sets	% of parameter sets
fails in wildtype	homogeneous	45,141	75.25
	partly well defined	2,705	4.51
	pattern except WER	45	7.5e-2
	pattern except WER and wer	3	5.0e-3
	pattern except CPC	514	0.86
	pattern except GL3c	3,240	5.40
	pattern except MYB23	33	5.5e-2
	pattern except EGL3c	792	1.32
	pattern except diffusing proteins	385	0.64
	no pattern	3,231	5.39
fails in scm mutant	homogeneous	903	1.51
	pattern does not match data	2998	5.00
total:		59,990	100

Figure S3-2. Breakdown of the reasons for failure of the unsuccessful parameter sets.



S4 File

Supporting information for Section 3.4, Table 8, of main manuscript.

Table S4. Successful parameter set numbers. Parameter set values for all parameter sets are available on GitHub [\[ref\]](#).

number of multiple binding site reactions removed	0	1			2			3
		multiple binding site removed			multiple binding site remaining			
WER transcriptional repression	all	<i>CPC</i>	<i>MYB23</i>	<i>WER/MYB23</i> <i>complex</i>	<i>CPC</i>	<i>MYB23</i>	<i>WER/MYB23</i> <i>complex</i>	none
cortical signal only	0	0	0	0	0	0	0	0
cortical signal and CPC	0	0	0	0	0	8340 9625 19016	0	0
cortical signal and CPC complex	3423	984	578	4615	0	4615	578	0
	3905	1985	4209	5034		5034	984	
	4209	2052	4513	6857		6857	1344	
	4634	3905	6055	10532		8558	1450	
	6365	4209		10715		9994	4209	
	10330	4634		11615		10532	10388	
	15122	4789		12202		10715	17988	
	15348	6365		12518		11615	19913	
	18537	8725		15280		12202		
	18878	12717		19016		12518		
		18878		19527		14539		
				19547		15280		
						19016		
						19527		